

FIGURE 6-20. The results of a countercurrent distribution separation of four closely related variants of the peptide antibiotic actinomycin C. Because of their slightly different distribution ratios in methyl butyl ether and 1.75% aqueous solution of sodium naphthalene- $\beta$ -sulfonate, the four components are separated slowly into four regions on the apparatus. See H. Brockmann and H. Grone, Chem. Ber. **87**, 1039 (1954).

#### 6-4 PHASE RULE

##### The Basic Idea

In a system with a given number of components, the number of variables that can be altered independently without creating or destroying phases can be shown to be related to the number of phases present in the system. This relationship is known as the phase rule. Consider a general one-component phase diagram, like Figure 5-7. We saw in Section 5-7 that with only one phase present, both  $P$  and  $T$  could be varied independently without producing any phase changes. Two phases could coexist only at points along one of the lines linking  $P$  and  $T$  through the Clapeyron equation. Finally, three phases can coexist only at the triple point. Neither  $P$  nor  $T$  can be changed without first eliminating one phase. The empirical relationship between the number of phases  $p$  and the number of independent variables or degrees of freedom  $f$  is

$$f = 3 - p \quad (5-21)$$

A two-component system is not as easy to diagram, since there are three independent variables: pressure, temperature, and concentration. The

Bi-Cd diagram of Figure 6-21 can be thought of as an isobaric slice through a full three-dimensional graph in  $P$ ,  $T$ , and  $X_{\text{Cd}}$  at 1 atm pressure. The change of the diagram with pressure is extremely slight in this condensed-phase system, but it is there in principle.

At a  $P$ ,  $T$ , and concentration represented by point  $a$  in the figure,  $P$ ,  $T$ , and  $X_{\text{Cd}}$  can all be varied independently without altering the number of phases. But if the temperature is lowered to that of point  $b$ , then the solution is saturated in Bi, and crystallization of a second phase begins. As the temperature is lowered still further, and as more Bi comes out, the solution becomes richer in Cd and its concentration follows the solubility curve from  $b$  to  $e$  and finally to  $h$ . As long as there are two phases in equilibrium, there are only two degrees of freedom:  $P$  and either  $T$  or  $X$ . At  $413^\circ$ , the solution becomes saturated in Cd as well as Bi, and crystals of both metals begin to form. With three phases in equilibrium, the system is locked at the eutectic point  $h$  and has only pressure left as an independent variable. Any attempts to raise the temperature are frustrated by the utilization of the heat supplied to melt solid Bi and Cd, until all of the Cd is exhausted. Only then can the temperature rise, in what is now a two-phase situation. Any attempts to lower the temperature result only in hastening the solidification process of the liquid, and only after it has disappeared can the temperature of the two-phase mixture of crystalline Bi and Cd be cooled, along the line  $g, j$ .

The empirical formula for the number of degrees of freedom in the two-component system is  $f = 4 - p$ . Comparing this to the one-component case, one might guess that the general phase relationship is  $f = c + 2 - p$ , where  $c$  is the number of components. This turns out to be correct, and is the usual expression for the phase rule.

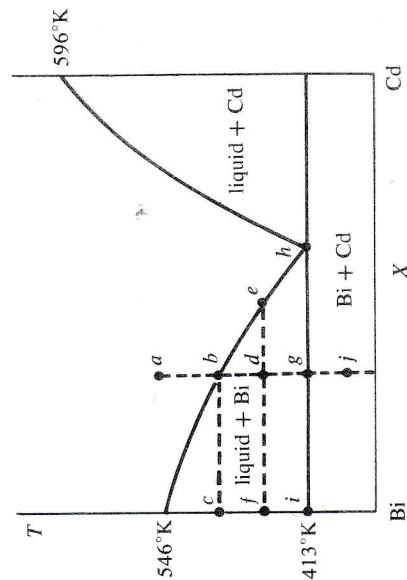


FIGURE 6-21. Temperature-composition plot for Bi and Cd. For explanation of points (a)-(j), see text.



### Derivation of the Phase Rule

The number of degrees of freedom a system may possess is just the number of independent variables that it takes to describe the system. From a mathematical point of view, the number of independent variables is the total number of variables minus the number of restraining conditions. The expression for the total number of variables is easy. In each phase, the mole fraction of each component must be specified, so that for  $p$  phases and  $c$  components, there are  $pc$  mole-fraction variables. In addition, there are the two addition variables of temperature and pressure, giving a total of  $pc + 2$  variables.

There are two basic types of restraining equations: the mole fractions in each phase sum to unity, and the chemical potential of each component must be the same in all phases. Thus there are  $p$  equations specifying that the mole-fraction sum in each phase is 1:  $\sum_j X_j^\alpha = 1$ . For each component, there are  $p - 1$  equations establishing the equality of chemical potentials in all phases:  $\mu_j^\alpha = \mu_j^\beta = \dots = \mu_j^p$ . There are  $c(p - 1)$  equations of this sort. The total number of restraining equations is therefore  $p + pc - c$ . Subtracting the number of equations of restraint from the number of total variables produces the number of *independent* variables:

$$f = pc + 2 - (p + pc - c) = c + 2 - p \quad (6-79)$$

[Parenthetically, this is of the same form as the expression relating the number of faces ( $f$ ), edges ( $c$ ), and vertices ( $p$ ) in a polyhedron. Is this only coincidence?]

### Number of Components

One important consideration when using the phase rule is to understand what is meant by the number of components in the system. The variable  $c$  is the number of chemically independent species necessary to describe the composition of every phase in the system. As in the derivation of the phase rule, the number of independent species is the total number of chemical species involved minus the number of restraining equations. In this case, the restraining equations turn out to be the equations of chemical equilibrium. To see what this means, consider the following examples.

In a system containing  $\text{PCl}_3$ ,  $\text{PCl}_5$ , and  $\text{Cl}_2$ , there are three chemical species. They are related, however, by the equilibrium expression  $\text{PCl}_5 \rightleftharpoons \text{PCl}_3 + \text{Cl}_2$ ; given any two mole fractions, the third can be calculated from a knowledge of the equilibrium constant. In such a system, there are only two independent components. One could retain all three as components and add the equilibrium expression to the list of equations of restraint, but it is easier to use such equilibrium expressions to reduce the number of components. In the case of liquid water, it is known that water may associate

with itself to form dimers, trimers, and large polymers. However, each of these associations is governed by an equilibrium equation, so that only one independent component is present. On the other hand, no known equilibrium exists between water and ethanol, so that a system with these two species would be a two-component system.

More than one phase may be involved in such considerations, as in the case of calcium carbonate and calcium oxide, both solids, with carbon dioxide, a gas. Even though each species is in its own phase, they are still linked by the equilibrium reaction  $\text{CaCO}_3 \rightleftharpoons \text{CaO} + \text{CO}_2$ . Even though there are three separate phases involved, there are only two components in the system.

The case of water, ethanol, and ethylene is not as clear. There is a reaction linking the three:  $\text{C}_2\text{H}_4 + \text{H}_2\text{O} \rightleftharpoons \text{C}_2\text{H}_5\text{OH}$ . However, the important point to be made is that equilibrium *must be attained* in order for the restraining equation to cancel out a variable. At room temperatures, this reaction proceeds extremely slowly, so that in most experiments equilibrium is never reached, and the dependence of the third species on the other two is never really established. Thus at room temperatures this is an effective three-component system. At elevated temperatures where equilibrium is more quickly achieved, the system behaves like a two-component system. Water offers another example of such a behavior; in the absence of a suitable catalyst, hydrogen and oxygen do not form water in a time comparable to that in which the experiment is conducted, nor does water break down to reach equilibrium with the gases. A system of hydrogen, oxygen, and water behaves like a three-component system, until a catalyst is added which permits equilibrium to be established rapidly.

### 6-5 TWO-COMPONENT SYSTEMS: LIQUID IMMISCIBILITY

The phase relationships in binary, or two-component systems, are easiest to illustrate and of the most general use. Aside from the intellectual challenge of plotting in four dimensions, three-component systems are the concern chiefly of the metallurgist. We shall look at phase equilibria involving two liquid phases, liquid and vapor, and liquid and solid. For two components there are three variables,  $P$ ,  $T$ , and  $X_j$ , which can be plotted as the three spatial axes. Whenever a two-dimensional plot is given, its place as one slice through the full three-dimensional graph should be kept in mind.

In any two-component system, the phase rule is

$$f = 4 - p \quad (6-80)$$

In an ideal solution of two liquids, there is complete miscibility at all concentrations and never more than one phase (see Section 6-1). But in nonideal solutions, the positive deviation may be so great that the liquid separates



into two phases: a solution of component  $A$  saturated in  $B$ , and another solution of component  $B$  saturated in  $A$ . It may not be possible to form one phase of intermediate composition.

An example of such behavior is the aniline-hexane system (Figure 6-22). At 25°C, only 10 mole % hexane can be added to aniline before the saturation point is reached and further hexane separates out as a second phase. If such a mixture is heated, more hexane will dissolve until finally the two liquids become completely miscible in all proportions at 60°C. This figure shows not only the compositions of the two immiscible solutions, but their relative mole amounts as well. Suppose that a solution of over-all composition  $X_c$  is brought to a temperature  $T_c$ . The composition of one of the two phases will be  $X_a$  and the other  $X_b$ , at the ends of a horizontal tie line. Moreover, the ratio of the total number of moles of the two solutions is given by the ratio of the opposite segments of the tie line:

$$\frac{n_a}{n_b} = \frac{CB}{AC} = \frac{X_b - X_c}{X_c - X_a} \quad (6-81)$$

This is the *lever principle*, and its proof is straightforward. Let  $n_a$  be the total number of moles in the phase of composition  $X_a$ , and  $n_b$  be that of phase  $X_b$ .

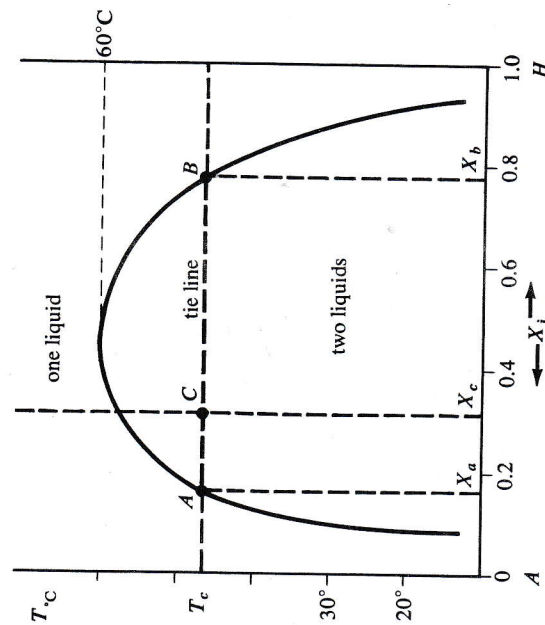


FIGURE 6-22. Solubility curve for aniline ( $A$ ) and hexane ( $H$ ) at moderate pressures. Below 60°C, two immiscible solution phases exist, of compositions given by the end points of a horizontal tie line at the temperature concerned. At 60°C the compositions of the two phases coincide and only one phase exists. This is called the upper consolute temperature.

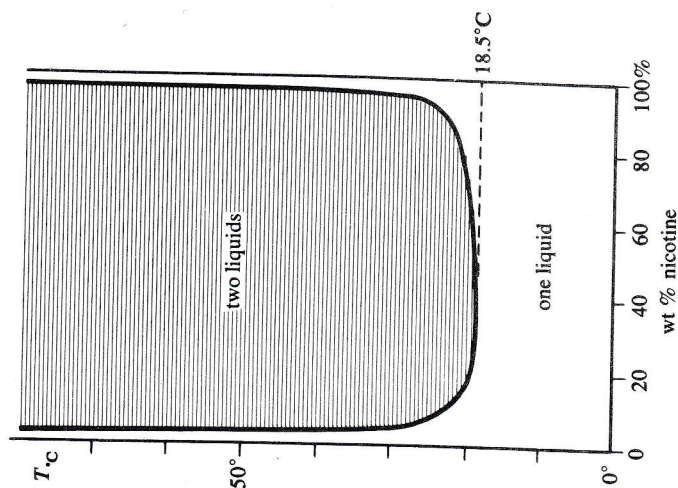


FIGURE 6-23. Triethylamine and water are completely miscible below 18.5°C, but separate into two immiscible solutions above this lower consolute temperature. The two-phase region is shaded with horizontal tie lines. What happens to the lever principle on a plot such as this of weight percent instead of mole fraction?

Let  $n_h$  be the total number of moles of hexane. The total amount of hexane will be the sum of that in the two phases:

$$n_h = n_a X_a + n_b X_b = (n_a + n_b) X_c \quad (6-82)$$

from which Eq. 6-81 follows at once. The lever principle is of general validity in the phase diagrams that we shall encounter.

Why do the two phases become miscible at 60°C? Hexane and aniline associate more readily with themselves than with each other. But as the temperature is raised, the kinetic energy of the molecules overcomes more and more of the energy barrier for association, and the solubility of each component in the other increases. At the so-called "upper consolute temperature" the saturation concentrations of the two phases become equal and the two phases become one. This behavior in a sense is like that of pure liquid and gas phases as the critical point is approached.

Triethylamine and water behave quite differently (Figure 6-23). At low temperatures they show negative deviation from ideality; the triethylamine-



water interaction is stronger than like-molecule interactions. Mixing is exothermic. But in turn, by Le Chatelier's principle, increasing the temperature should favor disassociation and the breakup of unlike-molecule associations. Above 18.5°C, this thermal disaggregation has proceeded to the point that the two components are no longer miscible in all proportions, and two phases can be obtained.

Nicotine and water show both phenomena (Figure 6-24), an upper and a lower consolute temperature. The tendency of unlike molecules to associate in all proportions at low temperatures has been broken up at 61°C, and a two-phase region begins. But by the time the temperature reaches 208°C, complete miscibility begins again. Le Chatelier's principle would lead one to predict that the mixing process for nicotine and water is exothermic at low temperatures and endothermic at high. Nicotine and water show negative deviation from ideality at low temperatures, and positive deviation at high.

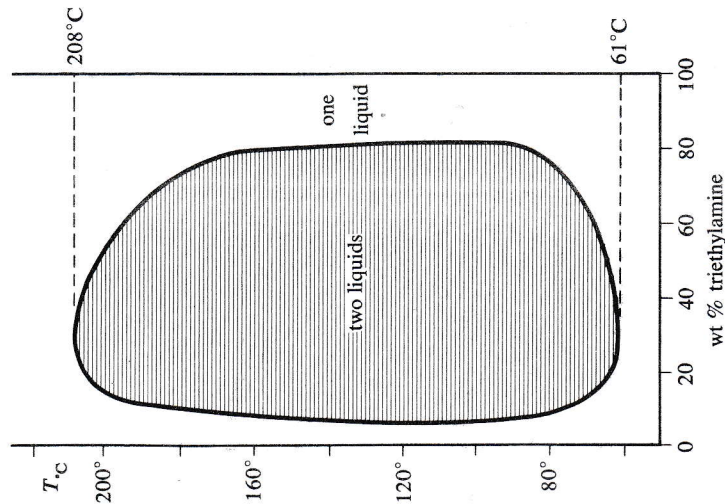


FIGURE 6-24. Nicotine and water show both an upper and a lower consolute temperature, with limited miscibility at intermediate temperatures. These data were collected from mixtures sealed in capillaries, so that pressure in fact rises with temperature. For the true pressure when the upper consolute point was measured, see Exercise 6-14.

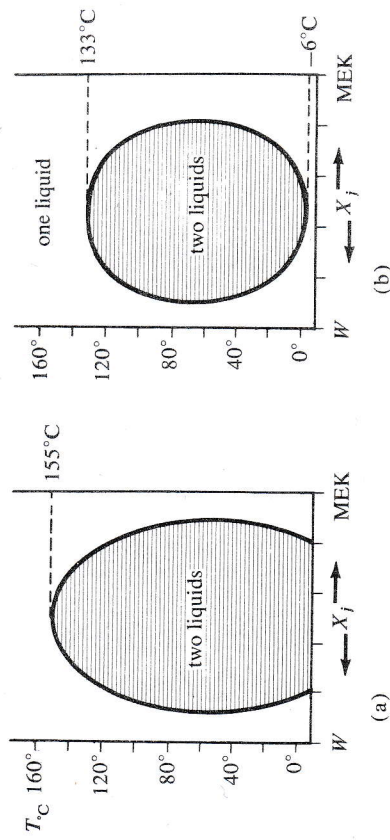


FIGURE 6-25. Miscibility of methyl ethyl ketone (MEK) and water ( $W$ ) at moderate pressures (a) and at 150 atm pressure (b). The vapor pressure of water at the upper consolute temperature of 155°C is approximately 5 atm, and the vapor pressure becomes 150 atm at 343°C.

The effect of pressure on the methyl ethyl ketone-water system is shown in Figure 6-25. This pair of compounds, like water and nicotine, shows negative deviation at low temperatures and positive at high. But in both ranges there is shrinkage on mixing. An increase in pressure, accordingly, favors the association process and increases the mutual solubilities. The size of the two-phase region shrinks as pressure rises, until at a sufficiently high pressure it disappears and the liquids are soluble in all proportions. The full phase diagram for this type of behavior is shown in Figure 6-26.

### 6-6 TWO-COMPONENT SYSTEMS: LIQUID-VAPOR EQUILIBRIUM

The coordinates of the three-dimensional liquid-vapor phase diagram which we shall build up are shown in Figure 6-27. The two  $PT$  plots which form the end faces have already been encountered. They are just the liquid-vapor pressure plots of Chapter 5, calculated from the Clausius-Clapeyron equation.

Now consider an isothermal slice, or a  $PX$  plot at constant  $T$ . The vapor composition will be represented as  $X_A^g$  and  $X_B^g$ , and the composition of the liquid by  $X_A^l$  and  $X_B^l$ . From Raoult's law, for ideal solutions,

$$P_T = X_A^l P_A^\bullet + X_B^l P_B^\bullet = P_B^\bullet + (P_A^\bullet - P_B^\bullet) X_A^l \quad (6-83)$$

This is the straight line in Figure 6-28, and has been seen before in Figure 6-1. The vapor will be richer in the more volatile component than in the liquid. The partial pressure of a component in the vapor is proportional to the mole fraction in the liquid, by Raoult's law. But it is also related to the gas phase



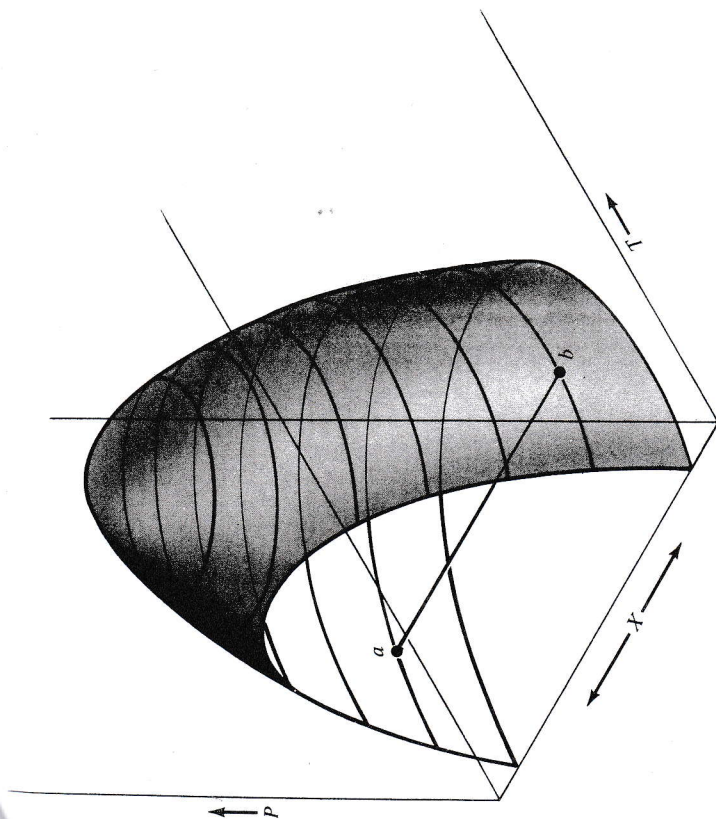


FIGURE 6-26. The complete pressure-temperature-composition diagram for two partially miscible liquids. Figures 6-22 to 6-25 are sections normal to the P axis. The ends of the tie line *ab* give the compositions of the two immiscible phases which will be present for any *P*, *T*, and *X<sub>j</sub>* point falling on the tie line. The relative molar amounts of the two phases will be given by the position of the *PTX* point on the tie line, in accordance with the lever principle. (*X<sub>j</sub>* is the over-all composition of both phases.)

composition by Dalton's law:

$$P_A = X_A^l P_A^\bullet = X_A^g P_T \tag{6-84}$$

From the previous two equations, the relationship between total pressure and gas phase composition can be found:

$$X_A^l = \frac{P_T - P_B^\bullet}{P_A^\bullet - P_B^\bullet} \tag{6-85}$$

$$X_A^g = \left( \frac{P_A^\bullet}{P_T} \right) \left( \frac{P_T - P_B^\bullet}{P_A^\bullet - P_B^\bullet} \right) \tag{6-86}$$

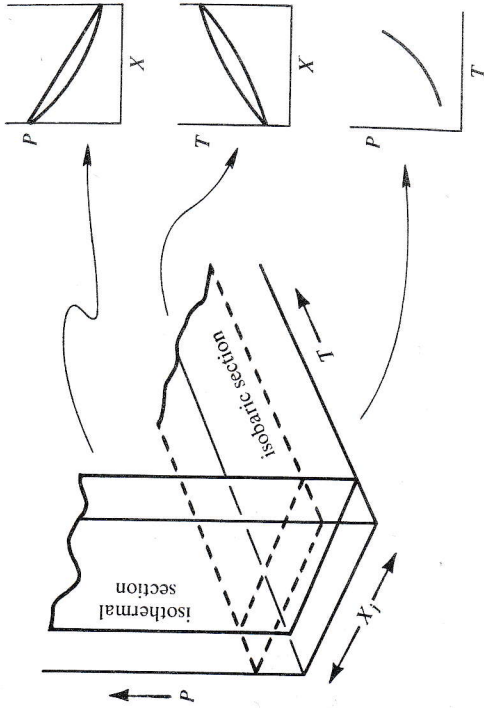


FIGURE 6-27. The pressure, temperature, and over-all composition axes of a full three-dimensional two-component phase diagram. Isothermal, isobaric, and pure-component sections are shown to the right.

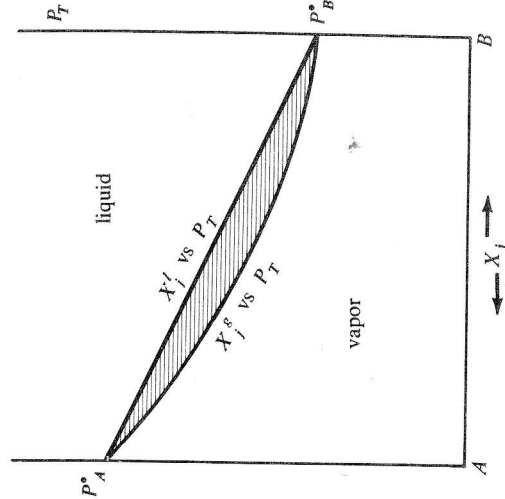


FIGURE 6-28. The composition of liquid (*X<sub>j</sub><sup>l</sup>*) and gas (*X<sub>j</sub><sup>g</sup>*) phases in an ideal solution as a function of total pressure *P<sub>T</sub>*. The two-phase region is shaded with horizontal tie lines.



This latter expression is the curved line in Figure 6-28. The region above the liquid line is a one-phase liquid region, and that below the vapor curve is a one-phase vapor zone, in both of which pressure and composition can be varied independently without creating a second phase. But any point between the curves represents a pressure and composition for which two phases, solution and vapor, will be present. The compositions of these phases are given at the ends of a tie line parallel to the  $X_j$  axis, and the relative molar amounts of liquid and gas phase are given by the lever principle.

Benzene and toluene form a nearly ideal solution, and their vapor pressure diagram is shown in Figure 6-29. If a liquid of the composition of line  $a-b-h$  is subjected to the pressure at point  $a$  in a closed cylinder, then no vapor will be present. When the pressure falls to that at point  $b$ , a vapor phase will begin to appear, richer in benzene than the liquid (composition  $c$ ). As the more volatile benzene predominates in the vapor, the liquid composition will fall along line  $b-d-f$  while the over-all gas phase composition goes from  $c$  to  $e$  to  $g$ . The last drop of liquid will have composition  $f$ , and below the pressure of the line  $g-f$  only the gas phase is present. If a liquid of composition  $a-h$  is exposed to an external atmosphere, then it will have in equilibrium with it a vapor of partial pressure equal to that of the line  $c-b$ . The phase rule is obeyed. For two components,  $f = 4 - p$ . But if variation is restricted to this isothermal plane then there is one less degree of freedom, or  $f' = 3 - p$ . When one phase is present, there are two degrees of freedom in this plane,  $P$  and  $X_j$ . But as long as both gas and liquid

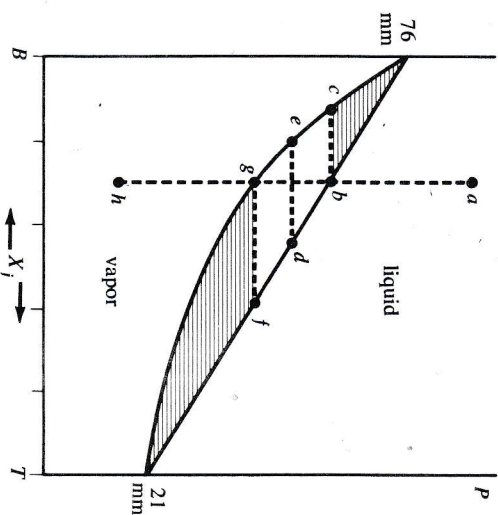


FIGURE 6-29. Composition of liquid and vapor as a function of pressure at 20°C for benzene (B) and toluene (T), which form a nearly ideal solution. The straight liquid-composition line has been seen before in Figure 6-1, but at 25°C.

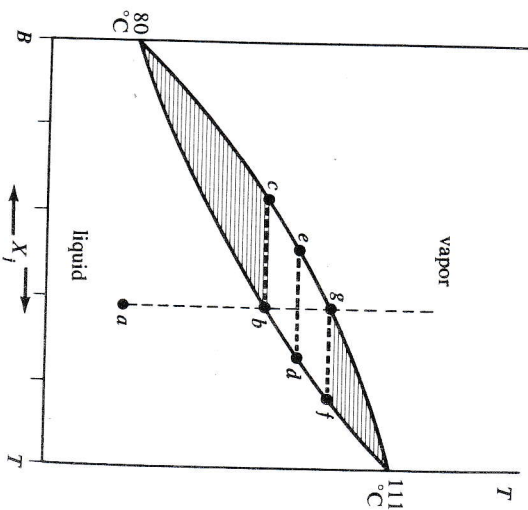


FIGURE 6-30. Boiling point diagram for benzene (B) and toluene (T) at 1 atm pressure. At any temperature, the upper curve gives the composition of the vapor and the lower curve the composition of the liquid with which it is in equilibrium.

coexist, there is only one degree of freedom, for the compositions of both phases are specified once  $P$  is given.

It is also possible from Eqs. 6-85 and 6-86 to calculate a  $TX$  plot of liquid and vapor pressures versus temperature for a fixed total pressure. The vapor pressures of the pure components are known functions of temperature,  $P_A^*(T)$  and  $P_B^*(T)$ , and can be varied while the total pressure is held constant. The resulting boiling point diagram is shown in Figure 6-30. The component with the higher vapor pressure, benzene, is naturally the one with the lower boiling point. If a liquid of composition  $a-b-g$  is heated in a closed piston at a constant external pressure, it will not show a vapor phase until the temperature rises to that of point  $b$ . The first vapor will have the composition of point  $c$ , and as the temperature is raised still higher (keeping the pressure constant), the vapor composition will rise from  $c$  to  $e$  to  $g$  while that of the liquid goes from  $b$  to  $d$  to  $f$ . At this point the composition of vapor equals that of the entire system and the last drop of liquid disappears. A liquid exposed to the atmosphere at the temperature of point  $a$  will have a vapor pressure less than the external atmospheric pressure, and point  $b$ , the boiling point, is that temperature at which the vapor pressure becomes equal to the atmospheric pressure. The lever principle again holds in calculating the relative molar amounts of liquid and vapor.

The full three-dimensional phase plot can be built up by studying a series of vapor pressure plots at different temperatures (Figure 6-31) and boiling



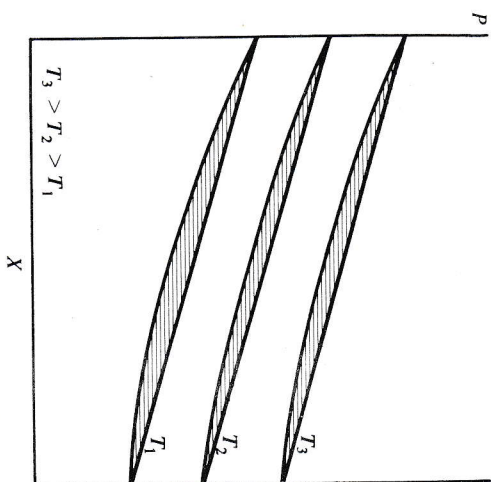


FIGURE 6-31. The rise of the vapor pressure curves to higher pressures as temperature is increased.

point plots at different pressures (Figure 6-32). As the temperature is raised, the vapor pressure is increased and the vapor pressure curves rise. As the pressure is increased, on the other hand, it becomes more difficult for molecules to escape to the gas phase, and boiling occurs only at higher temperatures. The complete diagram is shown in Figure 6-33. It consists of two surfaces: the upper giving liquid phase composition and the lower, gas surfaces:

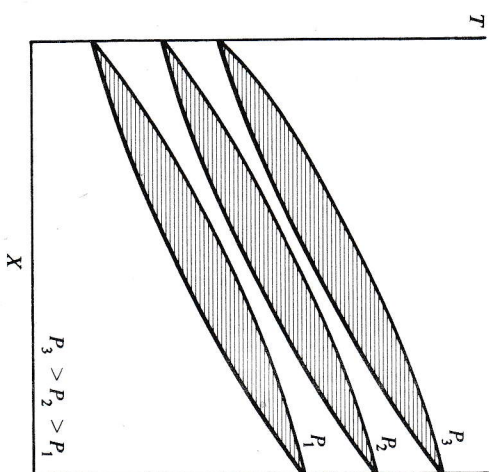


FIGURE 6-32. The rise of boiling point curves to higher temperatures as the pressure is increased.

phase. The regions above and below this pair of surfaces are one-phase zones with three degrees of freedom. But any point at a  $(P, T, X_1)$  between these surfaces represents a two-phase situation with gas and liquid compositions given by the intersections with the two surfaces of a line through this point and parallel to the  $X_j$  axis. The relative amounts of the two phases are inversely proportional to the distances from the over-all composition point to the intersections with the surfaces.

Two ideal liquids of different boiling points can be separated completely by the process of fractional distillation, illustrated in Figure 6-34. The process is simple, if tedious: if the initial mixture has a composition  $a$ , heat it to the boiling point at  $e$  and continue to heat it until the tie line is balanced ( $b-c$ ) and there are equal molar amounts of liquid and vapor. Separate the vapor and

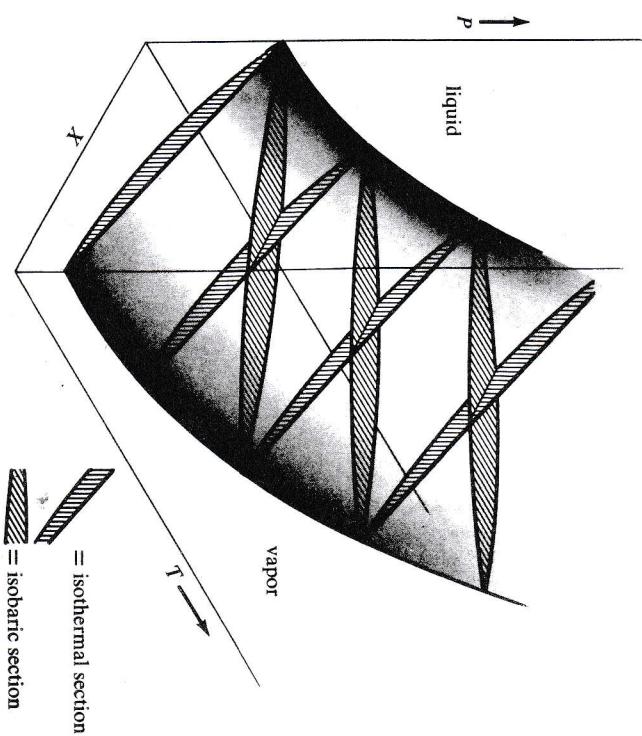


FIGURE 6-33. The complete pressure-temperature-composition phase diagram for vapor and an ideal two-component solution. The upper surface represents solution compositions, and the lower, vapor compositions in two-phase situations. At any over-all composition point between these surfaces, the compositions of vapor and liquid are found by extending a line through this point and parallel to the  $X$  axis until it touches the surfaces. The relative amounts of liquid and vapor are found from this tie line by the lever principle. At any  $P, T$ , and over-all  $X$  point which does not lie between these two surfaces, there will be only one phase present, liquid or vapor. Sections corresponding to Figures 6-28 through 6-32 are marked. Shading in these sections does not represent tie lines.



condense it. There will now be equal amounts of two liquids, one of concentration  $b$  and one of  $c$ . Heat the first again until half the material is vapor of composition  $d$  and half is liquid at  $e$ , then separate and cool. Treat the other half similarly to produce one fraction of composition  $f$  ( $=e$ ) and another of  $g$ . Combine the two central fractions. The end result of this two-stage process is one quarter of the original with composition  $d$ , one half with  $e$ , and one quarter with  $g$ . Now heat all three, separate, combine adjacent equal fractions, and repeat. The beauty of this process is that it can be carried out automatically in a bubble-cap fractionating still of the type in Figure 6-35. Vapor from one level bubbles up through the liquid of the level above and condenses, while liquid overflows back to the lower level. If mixture is fed in at the center, then the more volatile component flows out at the top (if the column is tall enough) while the less volatile liquid collects at the bottom. A simpler way to accomplish the same thing is to pack a column with glass beads, for which the continual condensation of vapor from below and reevaporation acts like a column of a great many smaller stages.

### Negative Deviation from Ideality

For negative deviation the vapor pressure is less than that expected for ideal solutions, and the complete vapor pressure-versus-composition plot is like that of acetone and chloroform shown in Figure 6-36. At the minimum in vapor pressure, the vapor and liquid compositions must be the same, and the two curves touch. The boiling point diagram shows a maximum (Figure 6-37). Any attempts to fractionate a mixture of acetone and chloroform of

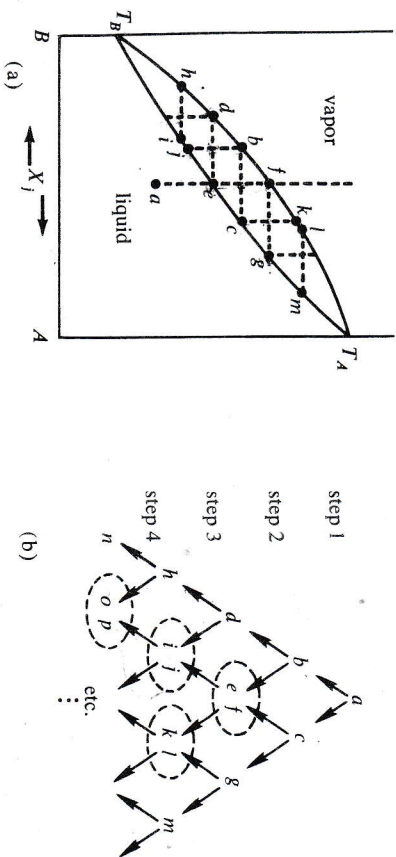


FIGURE 6-34. Fractional distillation. (a) Boiling point diagram; (b) fractionation and recombination scheme. The liquid fraction from one sample and the vapor from the adjacent one ( $e$  and  $f$ ,  $i$  and  $j$ ,  $k$  and  $l$ , and so on) are of approximately the same composition and are recombined before the next heating step. This fractionation scheme is logically equivalent to the countercurrent distribution one in Figure 6-18.

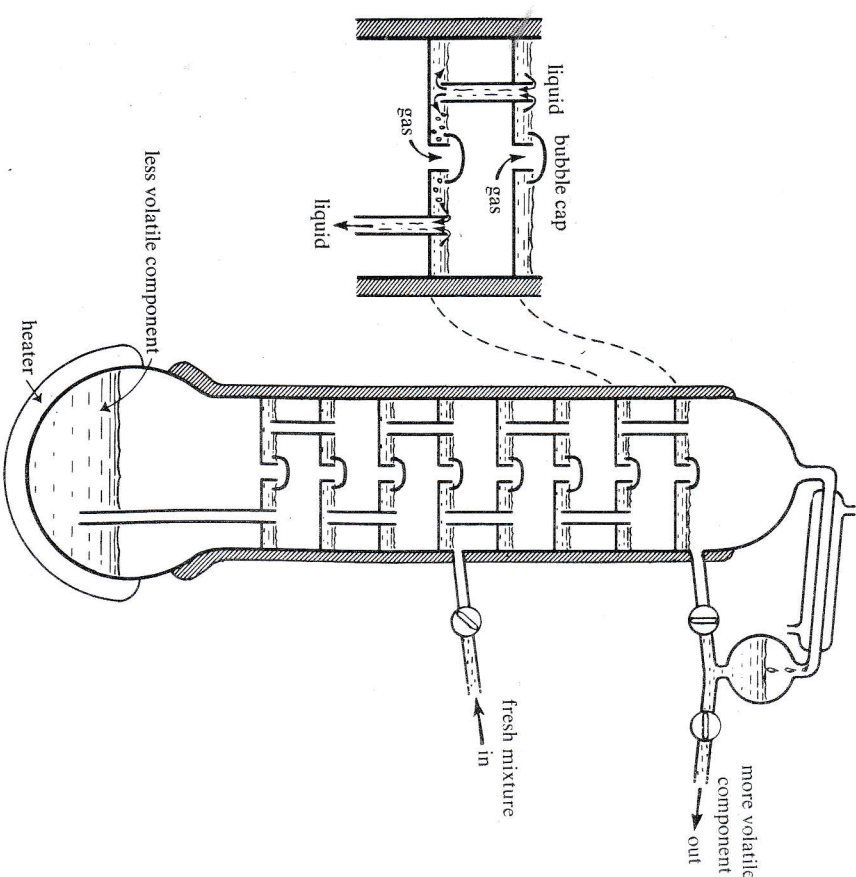


FIGURE 6-35. Bubble-cap fractionating column for accomplishing the processes of Figure 6-34 automatically. Vapor from one stage equilibrates with liquid in the stage above, and excess liquid returns to the stage below.

initial composition  $a$  by distillation will result in pure acetone and a constant boiling mixture, 0.65 mole fraction in chloroform, boiling at  $64.5^{\circ}\text{C}$ . Similarly, a starting mixture of composition  $d$  will yield only pure chloroform and the same "azeotropic" mixture (from "zein," to boil, and "atropos," unchanging).<sup>4</sup> Other systems which have such a maximum azeotrope are water and most of the inorganic acids, benzyl alcohol and  $m$ -cresol, and formic acid with either diethyl ketone or methyl  $n$ -propyl ketone. The three-dimensional  $PTX$  plot for negative deviation is like that for ideal solutions, but with a "trough" (Figure 6-38), along the bottom of which the two surfaces touch.

<sup>4</sup> This is the same Greek word that appears in "entropy," which was coined in the 1800's from "en-tropos" (involved in change), by analogy with "en-thalpein" (involved in heat) and the much older "en-ergon" (involved in work).



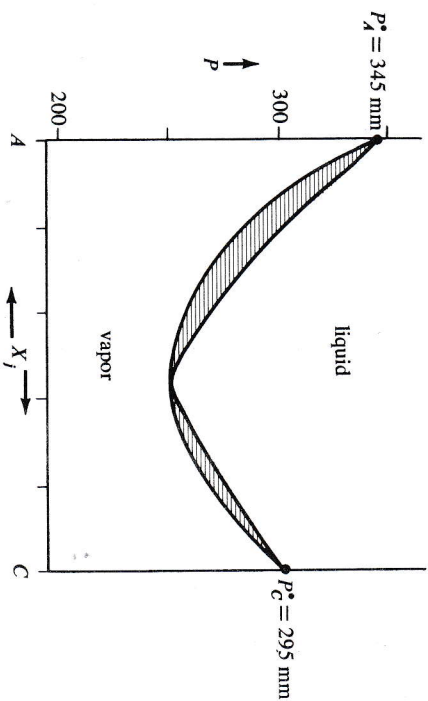
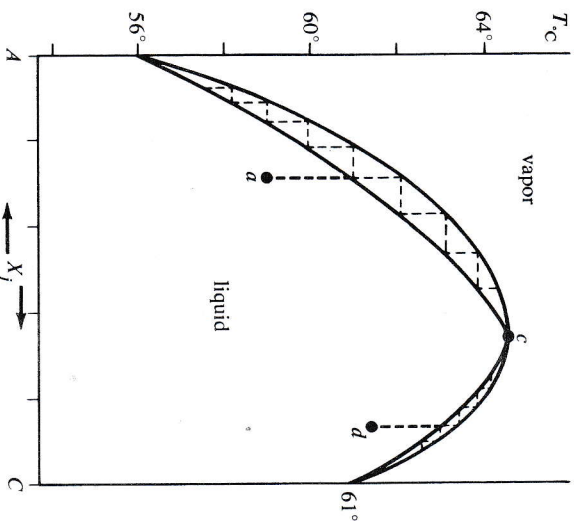


FIGURE 6-36. Vapor pressure diagram for a solution of acetone (A) and chloroform (C), showing strong negative deviation from ideality. The upper, liquid composition curve has been seen already in Figure 6-12. Acetone and chloroform associate more strongly with one another than with themselves, and the escaping tendency of a molecule to the vapor phase is less for a solution than for a pure component. Two-phase regions are shaded with horizontal tie lines.



$\Delta T, 64.5^\circ\text{C}$   
 $x_2, 0.65$

FIGURE 6-37. Boiling point diagram for the acetone-chloroform system, showing negative deviation from ideality. Fractional distillation of a liquid of initial composition a will yield pure acetone in the distillate and an azeotropic, or constant boiling, mixture of composition c. If the initial concentration is that of point d, then the end result will be pure chloroform and the same azeotrope c.

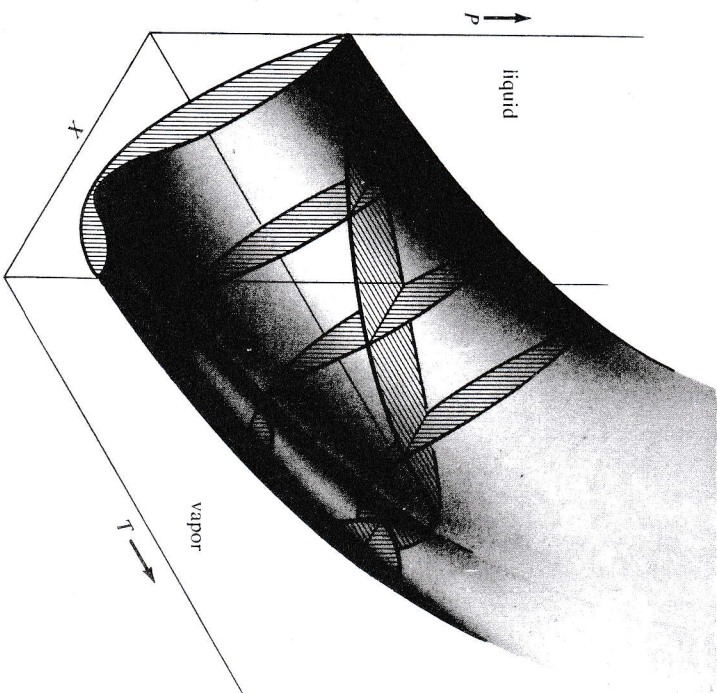


FIGURE 6-38. The full PTX phase diagram for a solution with negative deviation from ideality, analogous to Figure 6-33 for ideal solutions. Isothermal and isobaric sections corresponding to Figures 6-36 and 6-37 are shown. Shading in these sections is for structural emphasis, and is normal to the tie lines. The dashed line follows the azeotropic composition points, where the liquid and vapor composition surfaces touch.

**Positive Deviation From Ideality**

Positive deviation produces a vapor pressure curve with a maximum (Figure 6-39) and a boiling point diagram with a minimum boiling azeotrope (Figure 6-40). Ethanol, which normally boils at 78.4°C, also forms an azeotrope with water at 95.5% alcohol by weight, which boils at 78.1°C. It is impossible to prepare better than 95% ethanol starting from any more dilute solution of ethanol in water, and the common laboratory alcohol is this easily obtained azeotrope. A great many other liquid pairs form minimum boiling azeotropes because of molecular dissimilarity and reluctance to associate. These include water in combination with alcohols, hydrocarbons, ethers, esters, ketones, aldehydes, amines, and even organic acids. But alcohols themselves show negative deviation when mixed with hydrocarbons, esters, and alkyl halides.



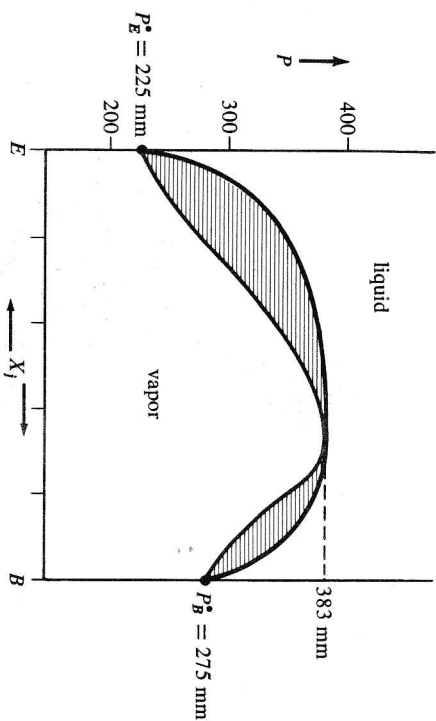


FIGURE 6-39. Vapor pressure diagram of a solution of ethanol (E) and benzene (B), showing positive deviation. The upper, liquid composition curve is analogous to the acetone-carbon disulfide curve of Figure 6-13.

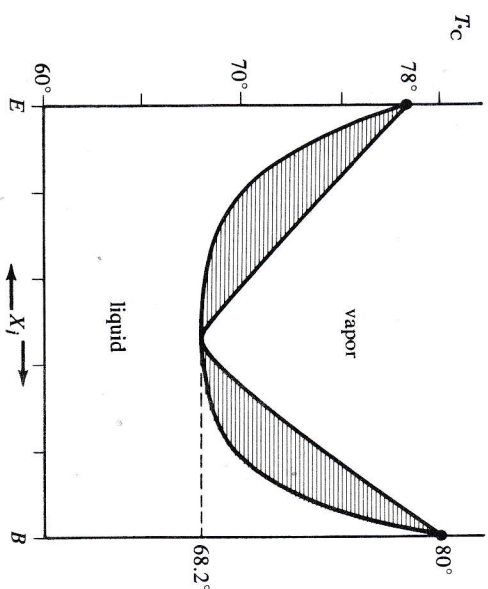


FIGURE 6-40. Boiling point diagram at 1 atm for the ethanol-benzene system, showing a minimum-boiling azeotrope. Fractionation of a solution to the left of the azeotropic composition would yield pure ethanol and a distillate of the constant azeotropic composition. From this figure and Figure 6-39, try to imagine the full PTX diagram for positive deviation, analogous to Figures 6-33 and 6-38.

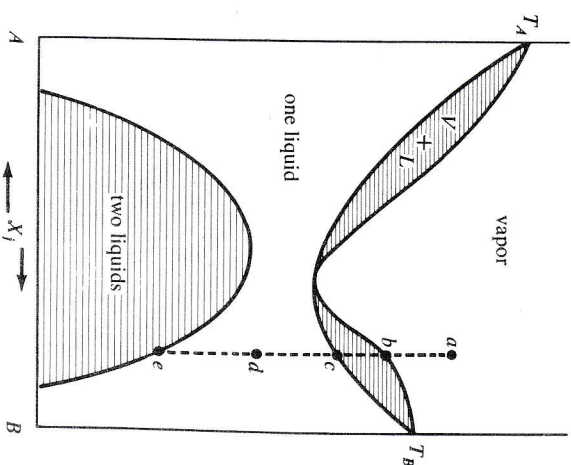


FIGURE 6-41. Liquid-vapor phase diagram at constant pressure for a solution which shows both positive deviation from ideality and partial liquid miscibility at lower temperatures. Liquid-vapor and liquid-liquid two-phase regions are shaded with horizontal tie lines.

If the positive deviation from ideality or reluctance of unlike molecules to associate is sufficiently great, then there may be immiscibility in the liquid phase like that of Figure 6-22, and an isobaric section may appear as in Figure 6-41. A vapor at  $a$  would begin to condense at  $b$  and form a two-phase system until  $c$ , at which point the last vapor would condense. There would be one liquid phase through  $d$  to  $e$ , where the temperature would have fallen so low that molecular motion was insufficient to keep the two components in association, and two immiscible phases would separate out. The effect of pressure on this diagram is shown in Figure 6-42. Decreased pressure lowers the boiling point curve and simultaneously encourages immiscibility, until just beyond Figure 6-42b the point is reached where the solutions remain immiscible all the way to the boiling point. In Figure 6-42c, vaporization occurs before the immiscible pair can be given enough thermal energy to make them mix. There will always be two liquid phases,  $\alpha$  being almost pure A with a little B, and  $\beta$  the reverse.



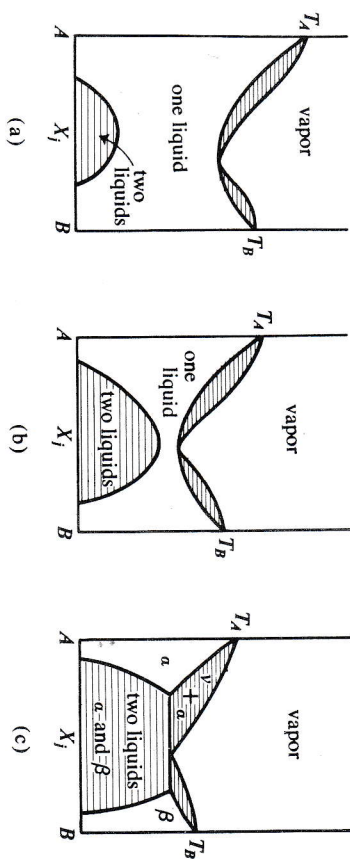


FIGURE 6-42. The effect of pressure on the phase diagram of Figure 6-41: (a) high pressure, (b) intermediate pressure, and (c) low pressure.

Water and butanol form such an extreme system (Figure 6-43). Much of this diagram should be obvious by now, but the three-phase point at  $h$  is new. As vapor at  $a$  is cooled, liquid condenses at  $b$ , and at temperature  $c$ , the vapor composition is at  $e$  and the liquid (phase  $\alpha$ ) at  $d$ . But at  $92.4^\circ\text{C}$ , a second liquid phase appears, immiscible with the first. At the instant that this second  $\beta$  phase first appears, the vapor is at composition  $h$  and the other  $\alpha$

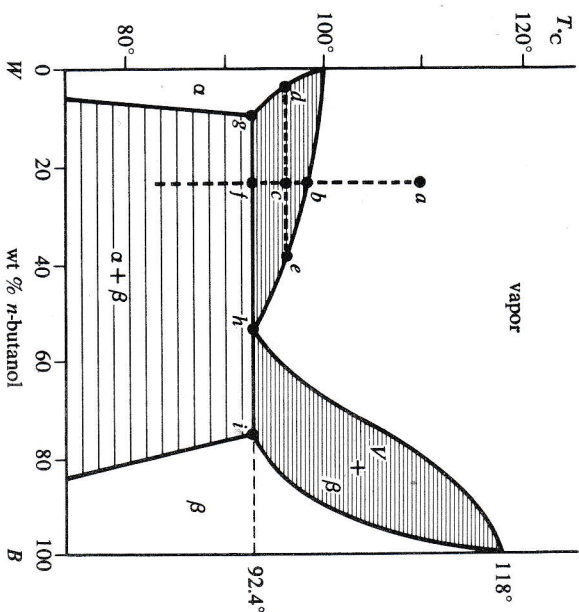


FIGURE 6-43. Isobaric phase diagram at 1 atm of the system of water ( $W$ ) and  $n$ -butanol ( $B$ ). The immiscible solutions  $\alpha$  and  $\beta$  vaporize before a high enough temperature can be reached to cause complete miscibility.

phase at  $g$ , with the ratio of vapor to liquid being the ratio of distances  $gf$  to  $fh$ . (Note that since the composition axis is in weight percent and not mole fraction, the lever principle gives the weight ratio of the two phases and not the mole ratio. You should be able to prove this by analogy with Eq. 6-82.) As long as three phases are present and in equilibrium, the temperature cannot be lowered. Any withdrawal of heat results not in a temperature drop but in a condensation of more vapor, in the "reaction":



This is consistent with the phase rule  $f = 4 - p$ , in that with three phases there is only one degree of freedom, and *none* within the isobaric section. As the last drop of vapor disappears, there remain two immiscible liquids for which the weight ratio of  $\alpha$  to  $\beta$  is  $f_i/gf$ . The butanol-water phase diagram at constant temperature looks like Figure 6-44. At very high pressures, the two immiscible liquids  $\alpha$  and  $\beta$  can be made miscible and the solubility curve will close over as in Figure 6-22.

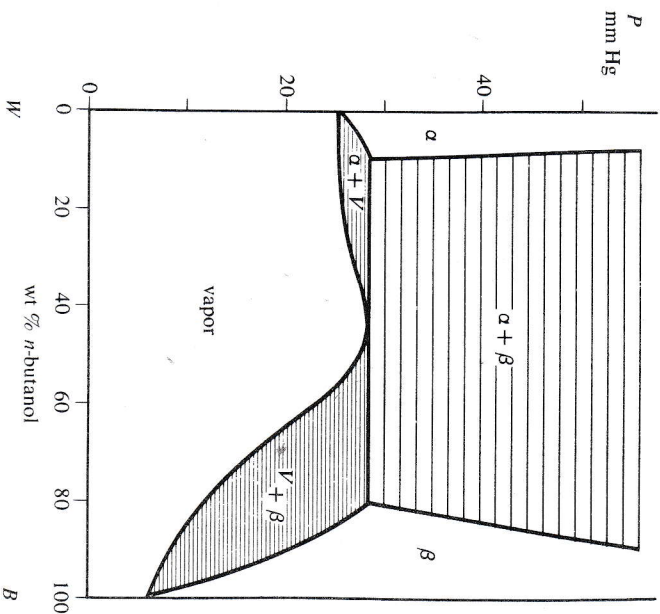


FIGURE 6-44. Isothermal phase diagram at  $25^\circ\text{C}$  of the  $n$ -butanol-water system.



**Complete Vapor-Liquid Phase Diagram**

All of the material in the last few sections can be summarized in a general three-dimensional *PTX* phase diagram for two components which show positive deviation from ideal solution behavior (Figure 6-45). The basic diagram shows two sets of surfaces. The first is the dome-shaped region of partial miscibility in the liquid phase (recall Figure 6-26). Outside this surface there is one liquid phase,  $p = 1$  and  $f = 4 - 1 = 3$ . Here there are three degrees of freedom:  $P$ ,  $T$ , and  $X_j$ . Within this surface there are two immiscible liquid phases whose composition is given by the termini of a tie line,  $\alpha$ - $\beta$ , and only two degrees of freedom exist. For once  $P$  and  $T$  are given, the compositions of the two phases are fixed.

The other surfaces in the diagram are the curved double-surface of liquid-vapor equilibrium analogous to Figures 6-33 and 6-38. A *PTX* point which falls between these surfaces marks a liquid-vapor two-phase situation. The compositions of the two phases are given by the intersections with the two surfaces of a tie line through the initial point and parallel to the  $X$  axis (see the line marked  $V-L$  in figure). The curves at which both surfaces come together at mole fractions of 0 and 1 (curves  $a_1$ - $b_1$ - $c_1$ - $d_1$ - $e_1$  and  $a_2$ - $b_2$ - $c_2$ - $d_2$ - $e_2$ ) are those obtained from the Clausius-Clapeyron equation for the respective pure components.

Five principal sections through the *PTX* plot are shown in Figure 6-46. The constant-pressure slice taken above the dome of immiscibility, (a), is analogous to the ethanol-benzene plot of Figure 6-40. The isobaric section taken below the point at which the immiscibility dome and liquid-vapor surfaces meet, (c), corresponds to the butanol-water system of Figure 6-43. The higher temperature isothermal section, (d), again is analogous to the ethanol-benzene diagram of Figure 6-39, and that at a lower temperature, (e), is like the butanol-water plot of Figure 6-44.

A similar *PTX* diagram for negative deviation has been given in Figure 6-38, but without the dome-shaped immiscibility feature it is much less interesting.

**Liquid Immiscibility Without Strong Positive Deviations**

It is possible to have limited miscibility in a solution in which the escaping tendencies of the components to the vapor differ only slightly from ideality. Then just as the butanol-water diagram, Figure 6-43, could be derived from Figures 6-22 and 6-40, so a combination of Figures 6-22 and 6-30 leads to Figure 6-47.

As a vapor of composition  $a$  is cooled, liquid phase  $\beta$  of composition  $c$  will begin to appear when the vapor is at point  $b$ . At the temperature of point  $d$  there will be vapor of composition  $e$  and solution  $\beta$  of composition  $f$ , in a

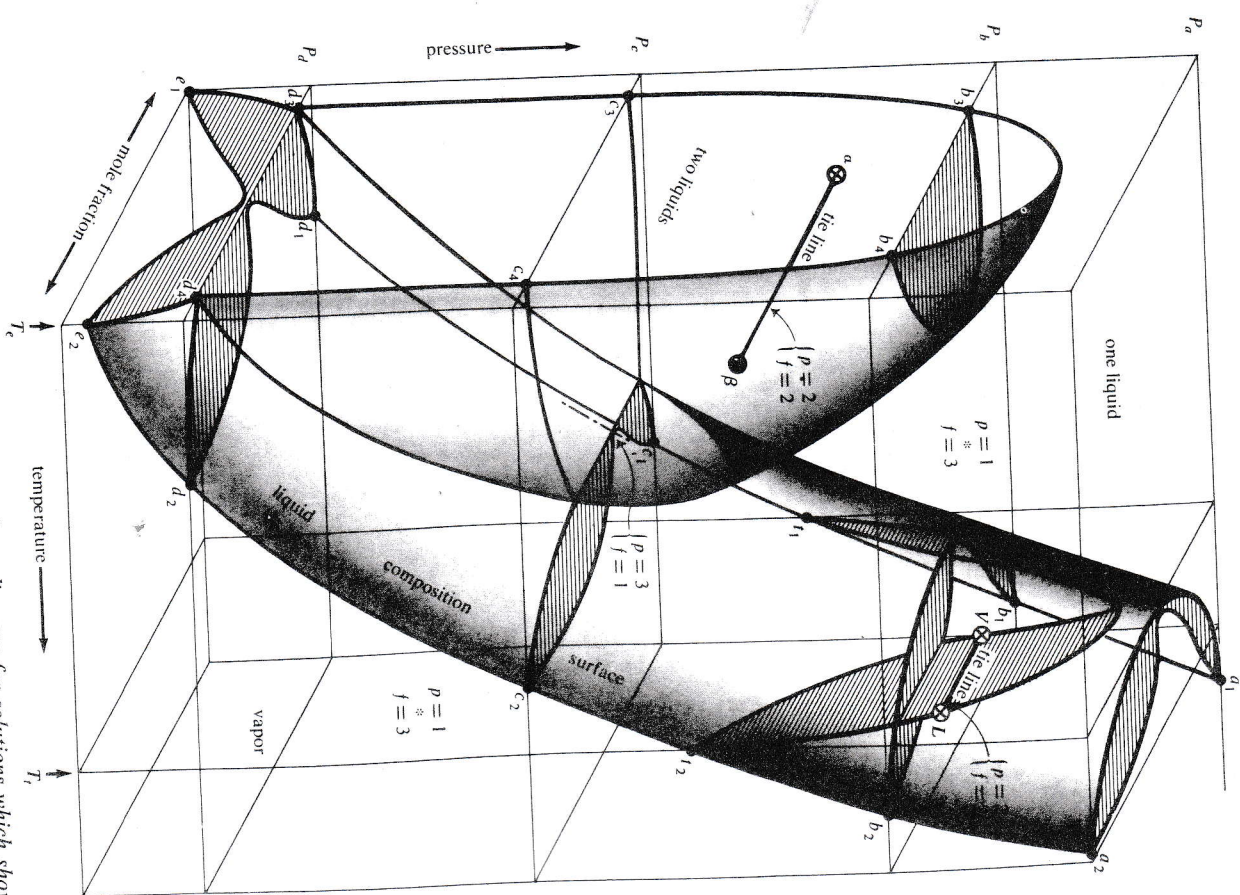


**FIGURE 6-45.** The complete liquid-vapor phase diagram for solutions which show positive deviation from ideality. Figures 6-39 through 6-44 are sections through this *PTX* plot. The dome of liquid two-phase immiscibility at the left is also seen in Figure 6-26. The curved, conical double surface at the right is the analog for positive deviations of Figures 6-33 and 6-38. At the various points marked,  $p$  is the number of phases present and  $f$  is the number of degrees of freedom, from the phase rule for two components:  $f = 4 - p$ . The end faces of the plot, for  $X = 0$  and 1, are the vapor pressure curves for the two pure components. Shading in the sections is for structural



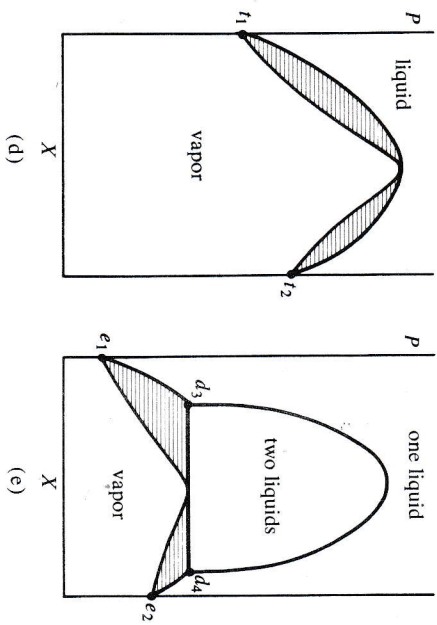
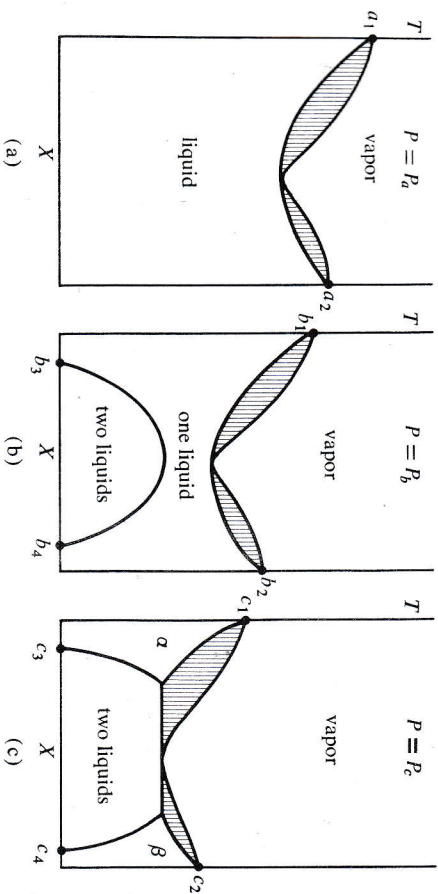


FIGURE 6-46. Sections through the full  $PTX$  diagram of Figure 6-45. (a)-(c) are at constant pressure, and (d) and (e) are at constant temperature. Shading is for emphasis only, in conformity with Figure 6-45.

vapor-to-liquid mole ratio of  $df/ed$ . Further removal of heat brings on the appearance of a second liquid phase,  $\alpha$ . But unlike the butanol-water system, the new phase is not richer than the vapor in the minority component of phase  $\beta$ . Instead, it is intermediate in composition between vapor and  $\beta$ . The reaction which produces this new phase is not

$$\text{vapor} = \beta + \alpha$$

(6-88)

SOLUTIONS

as in the butanol-water system, but is instead

$$\text{vapor} + \beta = \alpha$$

(6-89)

The new phase grows at the expense of both the old phases. If the butanol-water system is analogous to eutectic behavior in solid-liquid systems then this behavior is analogous to peritectic (see Figure 6-57). Only after all vapor has vanished can the temperature fall again for the two immiscible liquids.

Different behavior yet is observed starting from point  $h$ . Liquid phase  $\beta$  forms first at  $i$ , but at  $j$  phase  $\beta$  begins to dissociate according to the reaction

$$\beta \rightleftharpoons \text{vapor} + \alpha$$

$$\beta + \text{vapor} = \alpha$$

(6-90)

until only vapor and  $\alpha$  are left. At  $k$  the last vapor vanishes and only  $\alpha$  remains.

Steam Distillation

In purifying organic compounds, it is often desirable to distill a substance which is volatile, but which decomposes before its normal boiling point. One method is to distill at reduced pressure, but an alternative method is steam distillation.

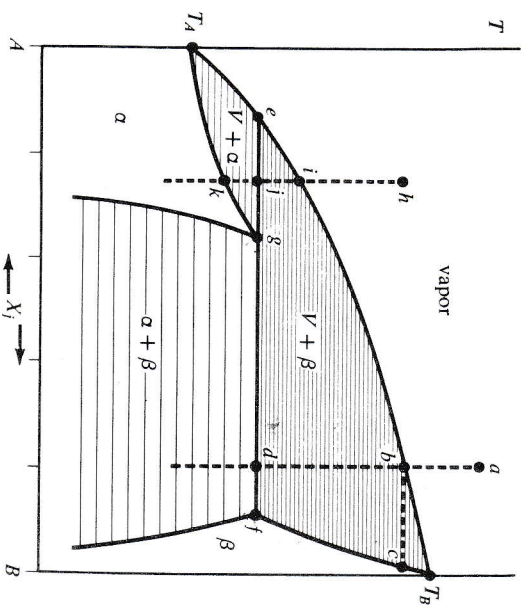


FIGURE 6-47. The liquid-vapor analog of peritectic behavior in solid-liquid systems (Figure 6-57).



The isobaric phase diagram for water and a typical organic liquid, nitrobenzene, is shown in Figure 6-48. Nitrobenzene and water form a constant boiling mixture of composition  $X_c$  at  $99^\circ\text{C}$ . If a steady supply of water as steam is provided, the temperature will remain at  $99^\circ\text{C}$  until all the nitrobenzene is used up. The mole ratio in the vapor will be that of the vapor pressures of the pure components at  $99^\circ\text{C}$ , which for water and nitrobenzene are 733 mm and 27 mm:

$$\frac{\text{moles water}}{\text{moles nitrobenzene}} = \frac{733}{27} = 27.1 \quad (6-91)$$

But with molecular weights of 18 and 123, the gram ratio of water to nitrobenzene is less:

$$\frac{\text{grams water}}{\text{grams nitrobenzene}} = \frac{733/18}{27/123} = 4 \quad (6-92)$$

Nitrobenzene can be distilled alone at  $211^\circ\text{C}$ , or can be distilled with water, with which it is immiscible, in a 1 to 4 weight ratio at  $99^\circ\text{C}$ . The ideal carrier

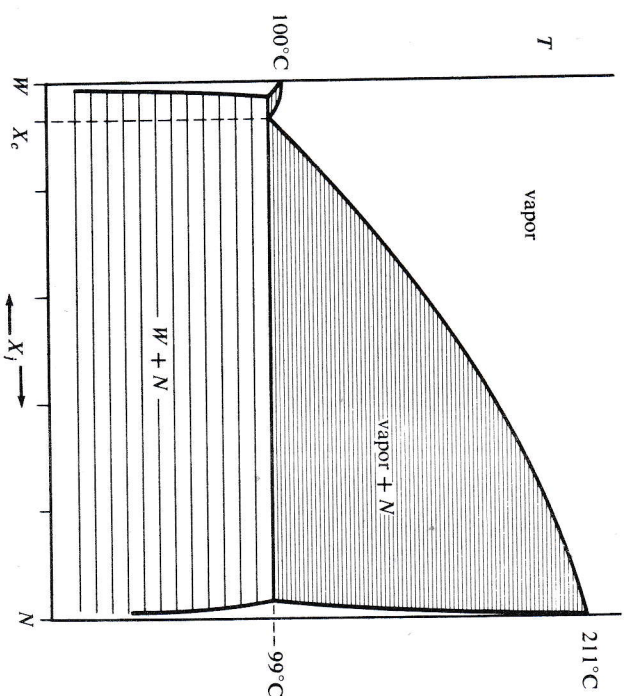


FIGURE 6-48. Phase diagram at 1 atm pressure for water ( $W$ ) and nitrobenzene ( $N$ ), to illustrate the process of steam distillation.

## SOLUTIONS

365

should be of low molecular weight and immiscible with the substance being distilled. Water serves admirably for many organic compounds.

Steam distillation can be used to determine rough molecular weights. As an example, terpinene steam distills at  $95^\circ\text{C}$  and 744 mm, in a distillate which is 55% terpinene by weight. At  $95^\circ\text{C}$  the vapor pressures of pure water and terpinene are 634 mm and 110 mm. The mole ratio is then

$$\frac{n_w}{n_T} = \frac{634}{110} = \frac{0.45/18}{0.55/M_T}$$

The approximate molecular weight of terpinene by this method is  $M_T = 127$ , to be compared with the true molecular weight of 136. Steam distillation can give a first order of magnitude figure for an unknown substance.

## 6-7 TWO-COMPONENT SYSTEMS: LIQUID AND SOLID EQUILIBRIA

Condensed phase diagrams are vitally important in studying and predicting the physical properties of solids, especially metals and alloys. But the most complicated such diagram can be broken down into a number of simpler types. What is more, all of these types have their analogs in the liquid-vapor diagrams which we have already seen. The chief difference is that changes in pressure have little effect upon equilibria between condensed phases, and all isobaric sections are virtually alike. The pattern of the solid state portion of Figure 6-45, if added to the left of the diagram, would extend up the  $P$  axis like the pattern in Christmas rock candy. In one isobaric slice, the phase rule for two components is  $f' = 3 - p$ .

### Structure of Solid Solutions

How can we form a solution in the solid state? In a solid, the atoms or molecules are packed in a regular array to form a crystal, and an alien "solute" atom or molecule can enter only by fitting into the interstices in the original crystal lattice or by replacing an atom or molecule of "solvent." Interstitial solutions or alloys are possible only if the added atoms are small, and substitutional alloys are possible only if the solute and solvent are of similar size and crystallize in much the same way. Copper and zinc in roughly equimolar amounts crystallize in a body-centered cubic (bcc) lattice in which the ratio of Cu to Zn can vary over considerable limits. The other type, interstitial alloys, can be represented by steel, which is an interstitial solution of carbon in iron, and by the alloy  $\text{Fe}_4\text{N}$ . In this latter compound, the iron atoms occupy the four sites per cell of a face-centered cubic (fcc)



lattice (Figure 6-50) while one nitrogen atom sits at the center of each cubic cell.

Body-centered, face-centered, and hexagonal close packing (hcp) are the three most efficient ways to pack structureless spheres, and are the most common crystal forms in metals and alloys. The most efficient packing of spheres in a plane is shown in Figure 6-49, where all neighboring spheres are touching, and the distance between centers  $d$  is the diameter of the sphere. A second equally well-packed layer can be fitted atop the first one so that its atom centers falls either at positions 2 or 3. If at 2, then a third layer can be placed at positions 3 or 1 with equal efficiency. If the sequence of layers is 1-2-1-2-1-2-1-2, then the atoms are in hcp. If the stacking order is 1-2-3-1-2-3-1-2-3-1-2-3, then the packing is called cubic close packing (ccp) or fcc. Both stacking sequences are illustrated in Figure 6-50, with the close-packed spheres replaced by much smaller ones for clarity. The numbers correspond to the layer numbering of Figure 6-49. Obviously many more layering schemes could be built. The metal americium, for example, crystallizes with a layer sequence 1-2-1-3-1-2-1-3-1-2-1-3-. But ccp and hcp are the most regular and by far the most common.

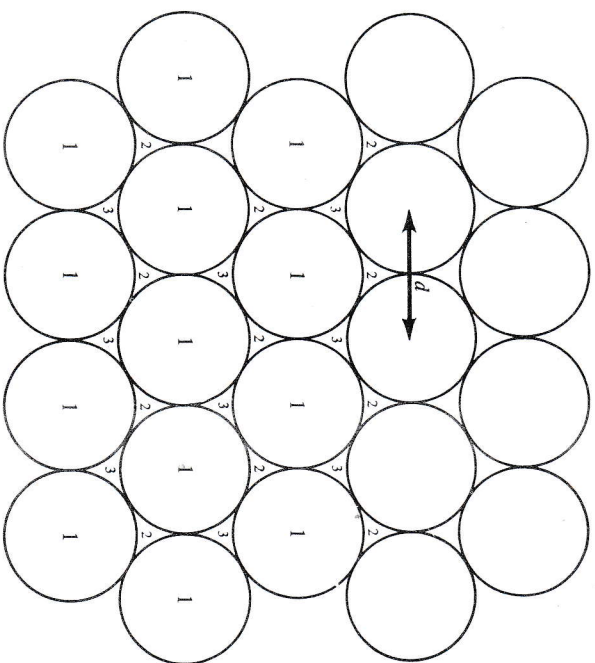


FIGURE 6-49. Close packing of spheres in a plane. A second plane could be packed most closely to this one by having its sphere centers at the positions marked 2 or 3. If at 2, then the third plane could be centered at positions 1 like the first plane, or at 3. The first choice leads to hexagonal close packing (hcp), and the second to cubic close packing (ccp).

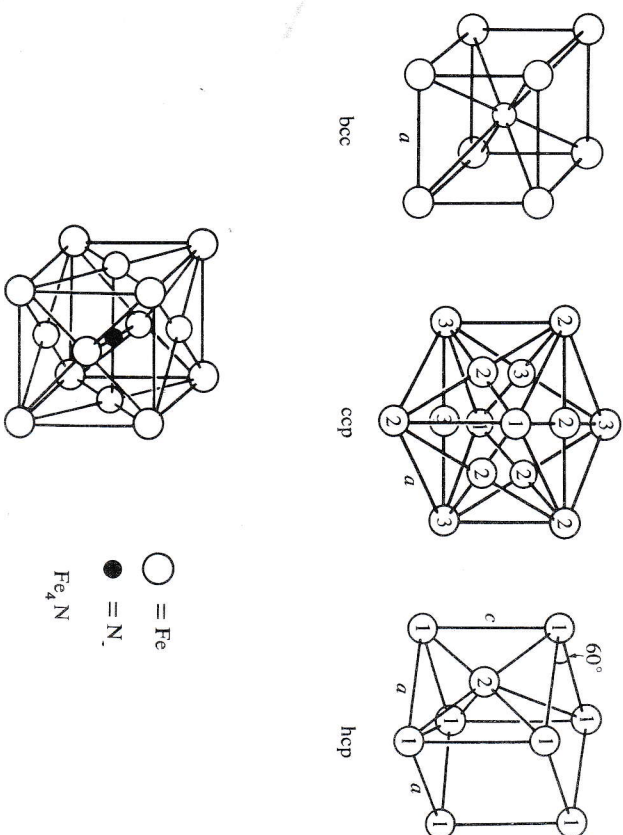


FIGURE 6-50. The three most common crystal packing schemes in metals and alloys, and the atomic arrangement in  $\text{Fe}_4\text{N}$ .

The basic unit cell edge in the ccp lattice,  $a$  in Figure 6-50, is  $\sqrt{2}$  times the sphere contact diameter  $d$ , and there are four atoms per cell. (The atom count will come out right if you remember that the number of atoms in one kind of environment, such as the corners, must be divided by the number of adjacent unit cells with which this kind of atom is shared. Thus ccp has eight corner atoms, each shared between the eight cells which meet at a given corner, and six face atoms, each shared between two neighboring cells.) In the ideal hcp lattice, cell edge  $a$  equals the sphere contact diameter  $d$ , and the axial ratio of  $c$  to  $a$  is  $2\sqrt{2}/\sqrt{3}$  or 1.633. There are two atoms per hcp cell. In both ccp and hcp, 26.0% of the solid is occupied by empty space between the packed atoms.

Body-centered cubic packing is only slightly more open, with 32% interstitial empty space. There are two atoms per cell, and the cell edge is  $2/\sqrt{3}$  or 1.15 times the sphere contact diameter. In what is to follow on liquid-solid phase diagrams, changes in kind and dimensions of crystal packing are crucial in producing the observed phase behavior. Table 6-2 lists crystal packing data for some of the elements whose phase behavior we shall examine. Note that the packing energy differences are so small that Na can pack in either hcp or bcc, and Ni in either ccp or hcp. Although Cu when pure is ccp and



TABLE 6-2 CRYSTAL STRUCTURES OF SOME METALLIC ELEMENTS

fcc (four atoms/cell) (measurements are in angstroms)		bcc (two atoms/cell)		hcp (two atoms/cell)	
Element	Ni	Cu	Pd	Ag	La
Atomic radius	1.24	1.27	1.37	1.44	1.86
Cell dimension $a$	3.53	3.61	3.89	4.08	5.30
hcp (two atoms/cell)					
Element	Na	Ni	Zn	Cd	
Atomic radius	1.86	1.24	1.33	1.49	
$a$	3.77	2.65	2.66	2.98	
$c$	6.15	4.33	4.95	5.62	
bcc (two atoms/cell)					
Element	Na	K	Mo		
Atomic radius	1.86	2.31	1.36		
$a$	4.29	5.25	3.15		
Arsenic hexagonal cell (six atoms/cell)					
Element	As	Sb	Bi		
Atomic radius	1.26	1.44	1.55		
$a$	3.70	4.31	4.55		
$c$	10.55	11.27	11.86		

Zn is hcp, in the approximately equimolar  $\beta$ -brass alloy they share a bcc lattice. The hexagonal arsenic-type structure of Table 6-2 is a distorted packing which to a first approximation can be thought of as a packing of layers in the sequence 1-2-x-3-1-x-2-3-x-1-x-2-3-x, where x- indicates an unusually wide gap between layers and where the layers themselves are distorted from simple close packing.

### "Ideal" Solid Solutions

If two substances crystallize in the same way when pure, and if their preferred crystal lattice dimensions are sufficiently close, then they can form a substitutional solid solution which satisfies the classical criterion for ideality—that all interatomic or intermolecular forces be *the same*. This is so for Cu and Ni (Figure 6-51), which when pure crystallize in ccp with cell dimensions 3.61 and 3.53 Å. Together they form a full range of ccp solid solutions with an ideal melting point diagram. This diagram should be compared to the benzene-toluene diagram of Figure 6-30. Au and Pt also form a nearly ideal solid solution, in the ccp lattice, and Sb and Bi do so in the hexagonal arsenic-type cell. It is possible to fractionate two such components by repeated melting and recrystallization, and the method is of some commercial importance.

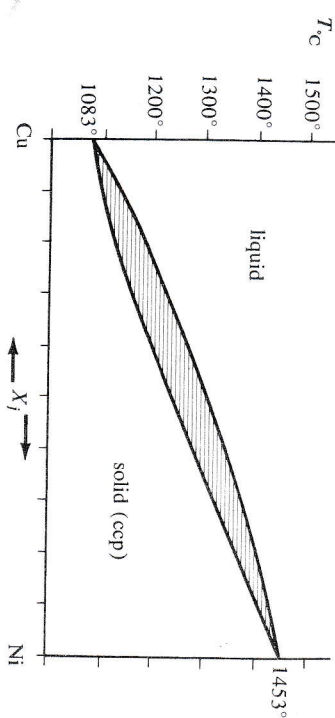


FIGURE 6-51. Melting point diagram for the Cu—Ni system, which shows nearly ideal solid solution behavior. The lower curve is the solid composition and the upper curve is the liquid composition in equilibrium with it at a given temperature. The interpretation, including the use of the lever principle, is identical to that of Figure 6-30. [From M. Hansen, *The Constitution of Binary Alloys* (McGraw-Hill, New York, 1958).]

If the atomic radii of two metals are sufficiently different, then it becomes difficult to accommodate one in the crystal lattice of the other, even though the lattices are of the same type. The ccp cell dimension of 3.89 Å for Pd is just enough greater than that of Ni so that too many Pd atoms stretch the Ni crystal lattice out of shape, and too many Ni atoms in Pd leave gaps which threaten the collapse of the lattice. There is therefore a greater escaping tendency of atoms into the melt from the strained lattice at intermediate compositions, and a lowering of the melting point. The melting point diagram, Figure 6-52, is a beautiful example of positive deviation, and should be compared with the ethanol-benzene boiling point diagram, Figure 6-40.

As and Sb form another example of positive deviation (Figure 6-53), and there have been reports of a region of immiscibility in the solid which would make the phase diagram resemble Figure 6-41 for the liquid-vapor system. Co and Cr,  $\text{KNO}_3$  and  $\text{NaNO}_3$  also form such solid solutions with positive deviation.

It is less easy to imagine a solid solution with negative deviation from ideality, or preferential association of unlike molecules. One example of this rare behavior is the mixture of *d*- and *l*-carvoxime,  $\text{C}_{10}\text{H}_{14}\text{NOH}$ . Each pure form melts at 72°C, but the 1:1 racemic mixture does not melt until 91°C (Figure 6-54). There are many examples known of association of unlike organic molecules in crystals, especially the stacking or pairing of ring structures, and the carboxime behavior may really be quite common. But little is known about phase behavior of organic crystals, or will become known until organic semiconductors become as interesting to the industrial solid state physicists as metallic systems.

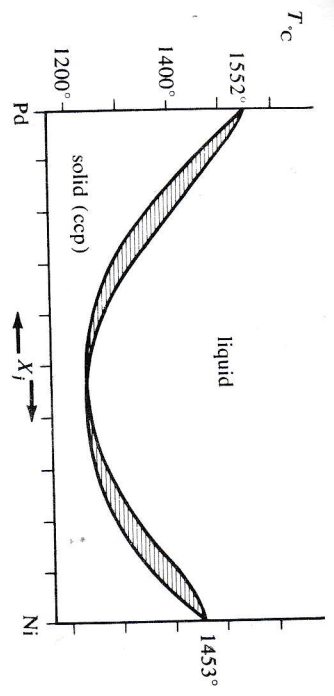


FIGURE 6-52. Positive deviation from ideality in the Pd-Ni solid solution system. (From Hansen.) Compare Figure 6-40.

**Solid Phase Immiscibility**

If the atomic or molecular dimensions of two substances which use the same lattice are too different, or if the substances prefer different lattices entirely, then the capacity of one to accept molecules of the other is finite, and there will be only a limited range of solubility. The Ag-Cu system (Figure 6-55)

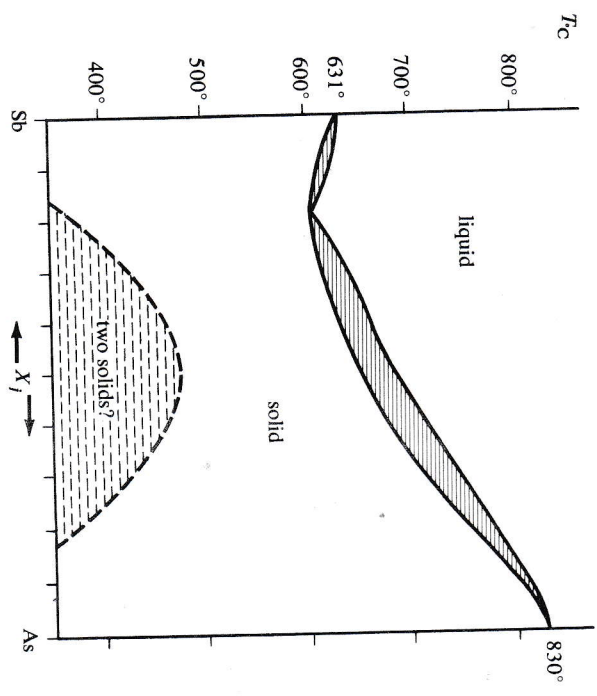


FIGURE 6-53. Positive deviation in the Sb-As system, with a suggested region of two-phase solid immiscibility. The right half of the diagram, near the pure As ordinate, was measured at elevated pressures to keep the arsenic from subliming. (From Hansen.) Compare Figure 6-41.

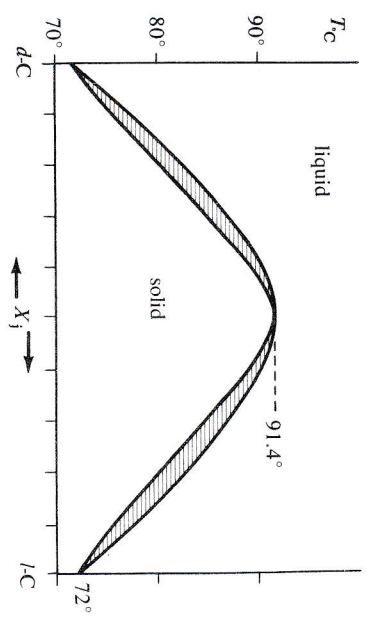


FIGURE 6-54. Negative deviation from ideal solid solution behavior in the system of the d- and l-isomers of carboxime. Compare Figure 6-37.

shows positive deviation and regions of immiscibility of two solid phases,  $\alpha$  and  $\beta$ . Both phases are ccp, but  $\alpha$  is a distortion of the Ag lattice with  $a = 4.08 \text{ \AA}$  for pure Ag, and  $\beta$  is a distorted Cu lattice with  $a = 3.61 \text{ \AA}$  when pure. The analogy with the butanol-water liquid-vapor diagram is exact and the interpretation is the same. Line  $u-v$  is the saturation curve for the liquid in the  $\alpha$  solid phase, and  $u-v$  gives the composition of the solid which

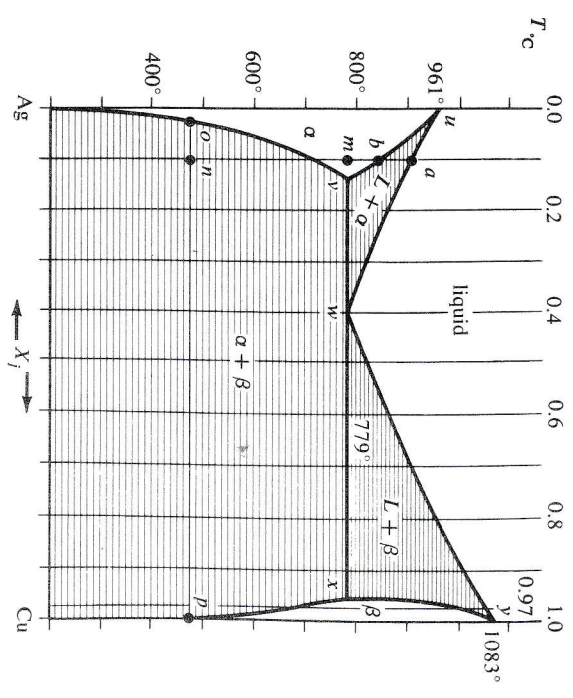


FIGURE 6-55. Limited solid solution miscibility in the Ag-Cu system. The vertical lines are the concentrations for the cooling curves in Figure 6-56. Two-phase regions, solid-liquid or solid  $\alpha$ -solid  $\beta$ , are shaded with tie lines. Compare Figure 6-43. (From Hansen.)



crystallizes out at a given temperature. Line  $u-w-y$  can also be thought of as the melting point line for the solid, and  $w$  is the eutectic, or "easily melted" point.

One of the ways of preparing such a phase diagram is to make up melts of different proportions of the two components, allow them to cool, and follow the cooling curve of temperature versus time at a constant rate of heat removal. A family of such curves for the Ag-Cu system is shown in Figure 6-56. Pure liquid Ag ( $X_{Cu} = 0.00$ ) cools above  $961^{\circ}\text{C}$  at a rate which is a function of its heat capacity. But at  $961^{\circ}\text{C}$  a second, crystalline phase appears and the temperature remains constant until all of the liquid is used up. The heat which diffuses away from the specimen is replaced by latent heat of fusion released upon crystallization. After the entire sample has crystallized, cooling again proceeds, but at a different rate reflecting the different heat capacity of the solid. The appearance of the solid will be that of large crystalline domains or grains of pure Ag, oriented at random relative to one another depending upon how the initial chance nucleations occurred.

A melt with 10 mole % Cu will have a different cooling curve. The slope will remain constant until approximately  $905^{\circ}\text{C}$ , when the first  $\alpha$  phase begins

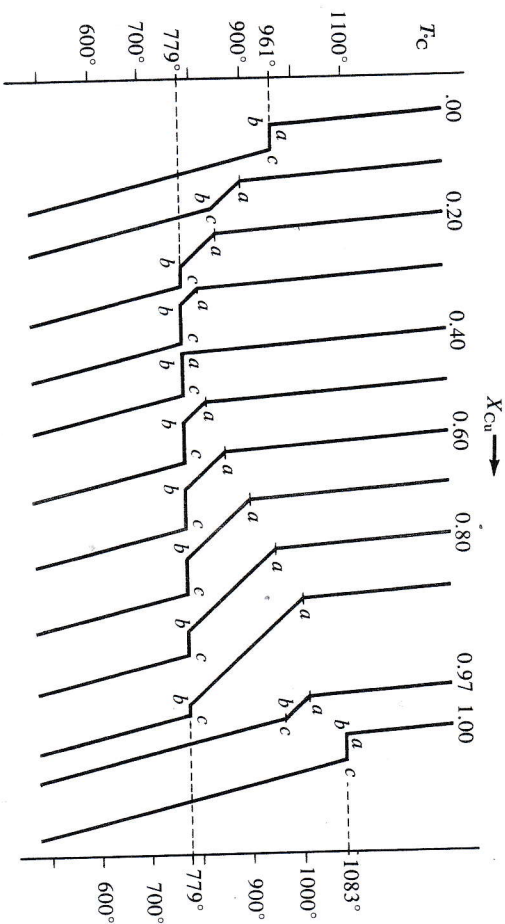


FIGURE 6-56. A family of cooling curves for the Ag-Cu system of Figure 6-55. The region from the top of the curve to point  $a$  represents cooling of the liquid. From  $a$  to  $b$ , the liquid is continuing to cool, but at a slower rate since a solid phase is crystallizing out and giving off its heat of fusion. Section  $b$  to  $c$  is a eutectic halt until the last liquid crystallizes, longer or shorter depending on how much liquid was left when the liquid composition reached the eutectic point ( $w$  in Figure 6-55). From  $c$  to the bottom of the diagram, the solid phase or phases are cooling. It is from information such as these curves provide that phase diagrams like Figure 6-55 are constructed.

to come down. The temperature will then fall more slowly, for latent heat of fusion is being released as phase  $\alpha$  crystallizes. At  $850^{\circ}\text{C}$  there is a second break in the cooling curve and in the absence of any more liquid to crystallize, the temperature drop in the solid  $\alpha$  phase is more rapid. These two cooling curve breaks define points  $a$  and  $b$  on the phase diagram. (Why, for pure Ag, does the onset of crystallization demand a temperature halt, while for the 10% mixture only a slowing of the temperature drop is observed? The facile answer is "The phase rule demands it." But do you really *understand* why?)

The 20 mole % cooling curve begins in a similar way; at  $860^{\circ}\text{C}$  there is a break in slope as phase  $\alpha$  begins to come out. As the temperature falls and as the Ag-rich  $\alpha$  phase crystallizes, the liquid becomes poorer in Ag and its composition falls along line  $u-w$ . At point  $w$  the liquid is saturated not only in the  $\alpha$  phase, but in the  $\beta$  phase as well, and *both* begin to crystallize simultaneously. Relative amounts of the three phases are given by the lever principle, as before. With three phases there are *no* degrees of freedom, and the temperature is stabilized at  $779^{\circ}\text{C}$ . This stabilization, marked  $b-c$  on the cooling curve, is called a eutectic halt. After the liquid is gone, then the mixture of  $\alpha$  and  $\beta$  phase crystals can be cooled at a new rate dependent upon their specific heats. The end product will be large crystals of  $\alpha$  which grew between  $860^{\circ}\text{C}$  and  $779^{\circ}\text{C}$ , embedded in a matrix of tiny crystals of  $\alpha$  and  $\beta$  which came down together during the eutectic halt.

The 30% Cu curve is similar, and provides another point on the  $u-w$  line on the phase diagram. The 40% line happens to go through the eutectic point  $w$  itself. There will be no crystallization at all until the eutectic temperature is reached, at which point both solid phases will come down simultaneously in a fine-grained eutectic matrix. The 50-90% cooling curves are like those at 20 and 30%, and help to map out curve  $w-y$ . But the solid now will be made up of large grains of  $\beta$  embedded in a eutectic matrix, rather than  $\alpha$ . The 97% curve is analogous to the 10%, and the pure Cu curve to the pure Ag.

The physical properties of the alloy are strongly influenced by the size of the grains, or crystalline domains. Large-grained metals are softer and more ductile; for a slip dislocation, once started by mechanical stress, can travel a great distance before it is halted at a grain boundary. If the domains could be made smaller, the metal would be harder. The eutectic matrix is just such a small-grained form, and it is for this reason that the alloy is harder and stronger than either pure silver or pure copper.

If a 10% Cu alloy is cooled slowly to point  $m$  in Figure 6-55, the resulting phase will be soft and ductile. If it is cooled rapidly, or quenched, to point  $n$ , it will still be ductile, for the  $\alpha$  phase, although now metastable relative to a mixture of  $\alpha$  and  $\beta$ , will not have had time to equilibrate. Equilibrium in solid solutions is reached slowly if at all. Eventually, the original crystalline



mass will separate into smaller grains of two phases, according to the reaction

$$\alpha_n = \alpha_o + \beta_p \tag{6-93}$$

where the subscripts refer to concentrations on Figure 6-55. This equilibrium mixture will now be much harder and less malleable. This is the process of age hardening, and can occasionally be seen as a crazed or crackle grain pattern on the surface of very old brass doorknobs. The other standard method of alloying to produce a hard metal was hinted at in passing when Fe<sub>4</sub>N was mentioned. In an interstitial alloy, the slip of one layer of metal atoms over another is impeded by foreign atoms like C or N which act like sand in the bearings. Whether by grain boundaries or intercalated atoms, the goal in hardening metals is to make the free passage of one layer of atoms over another difficult.

Peritectic behavior, in contrast to the eutectic behavior just discussed, is seen in the AgNO<sub>3</sub>-NaNO<sub>3</sub> system (Figure 6-57). The interpretation is analogous to that of Figure 6-47. As an  $\alpha$  phase solid at point  $a$  is heated, it begins to melt at point  $b$  to a liquid of composition given by the other end of the horizontal tie line. At the temperature of point  $c$ , the liquid has composition  $d$ , and the solid phase  $\alpha$ ,  $e$ . But at this "peritectic temperature" a rather strange behavior is observed. As more  $\alpha$  phase melts, liquid is formed,

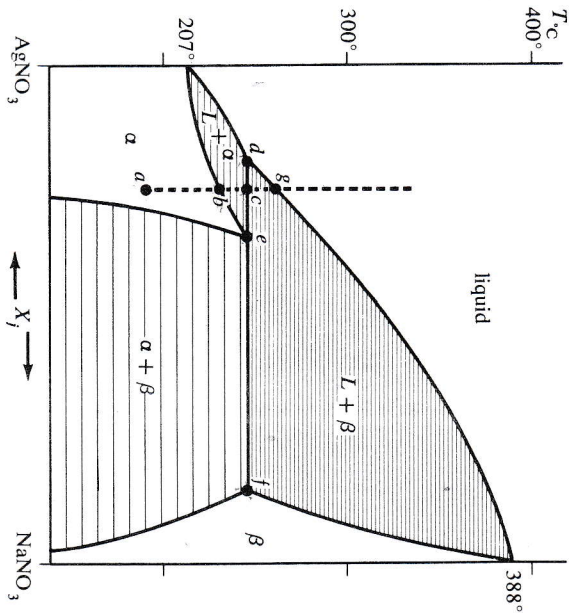


FIGURE 6-57. Peritectic behavior in a system with a range of compositions possible in the solid phases.

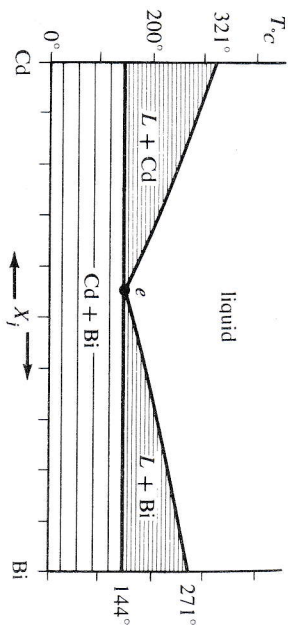


FIGURE 6-58. Simple eutectic diagram of the Cd-Bi system, with complete immiscibility of the two solid phases. Figures 6-52, 6-55, and this one form a progression of increasing incompatibility of each pure component in the crystal lattice of the other. (From Hansen.)

but so is a new solid phase  $\beta$ . The reaction is

$$\alpha = \text{liquid} + \beta \tag{6-94}$$

It is for this reason that this behavior is called peritectic, or "melting with change" behavior. What would a set of cooling curves for peritectic behavior look like, especially in the composition region between pure AgNO<sub>3</sub> and point  $e$ ?

Cd and Bi crystallize in totally different forms, Cd in hcp and Bi in the hexagonal arsenic lattice (Table 6-2). They are totally insoluble in one another in the solid state, and their phase diagram is shown in Figure 6-58. This is just the limit of the Ag-Cu diagram with the  $\alpha$  and  $\beta$  solubility zones flattened out against the vertical axes. The interpretation of the diagram is obvious. Point  $e$  is the eutectic point, where the solid melts to a liquid of the same composition. This behavior is also shown by KCl and AgCl (both the NaCl lattice, but unit cell distances of 6.29 and 5.55 Å, respectively), bromoform and benzene, and picric acid and TNT.

TABLE 6-3 TYPICAL EUTECTIC FREEZING MIXTURES

Mixture	$T_e$ (°C)
H <sub>2</sub> O and Na <sub>2</sub> SO <sub>4</sub>	-1.1
H <sub>2</sub> O and KCl	-10.7
H <sub>2</sub> O and NH <sub>4</sub> Cl	-15.4
H <sub>2</sub> O and NaCl	-21.1
H <sub>2</sub> O and NaBr	-28.0
H <sub>2</sub> O and CaCl <sub>2</sub>	-55



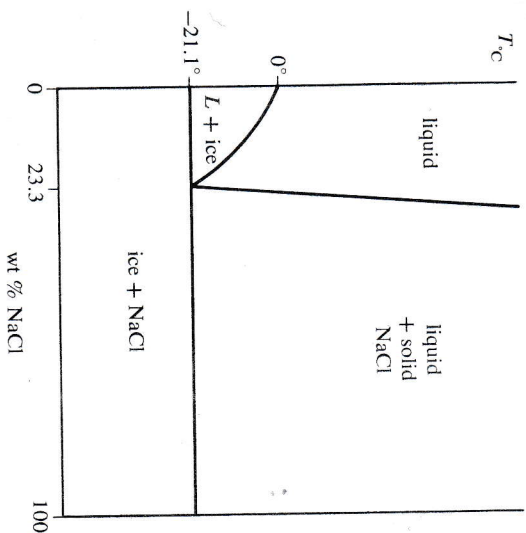


FIGURE 6-59. Eutectic diagram for a salt water freezing bath.

The eutectic halt is a useful means of maintaining a constant temperature. In the salt bath whose phase diagram is shown in Figure 6-59, as long as liquid, ice, and salt are all present, the temperature is fixed at the eutectic temperature of  $-21.1^{\circ}\text{C}$ . If heat is added, ice melts to compensate for it; if heat is withdrawn, more water freezes out from the solution. Table 6-3 shows some other freezing mixtures using water, and others involving acetone or other organic solvents are common.

**Complex Diagrams and Compound Formation**

The most complex phase diagram can be understood if it is broken down into the basic types discussed so far. Consider two substances *A* and *B* which associate readily with one another in the solid solution. Then their phase diagram might appear as Figure 6-60a. In the extreme case of association, an intermediate compound might be formed,  $AB_2$ , and the phase diagram would appear like two Cu-Ni diagrams side by side. Now suppose that the compound  $AB_2$  does not pack particularly well into the lattices of either *A* or *B*. Then the system would show positive deviation between *A* and  $AB_2$ , and  $AB_2$  and *B*, as in Figure 6-60b. In the extreme case there might even be immiscibility of  $AB_2$  with *A* and with *B* at lower temperatures, as in Figure 6-60c.

Only one step beyond this point brings us to the  $\text{Ti}_2\text{O}_3$ - $\text{TiO}_2$  diagram of Figure 6-61. This looks like two Ag-Cu diagrams side by side. There are three solid phases:  $\alpha$ ,  $\beta$ , and  $\gamma$ . The two-phase regions are marked. There

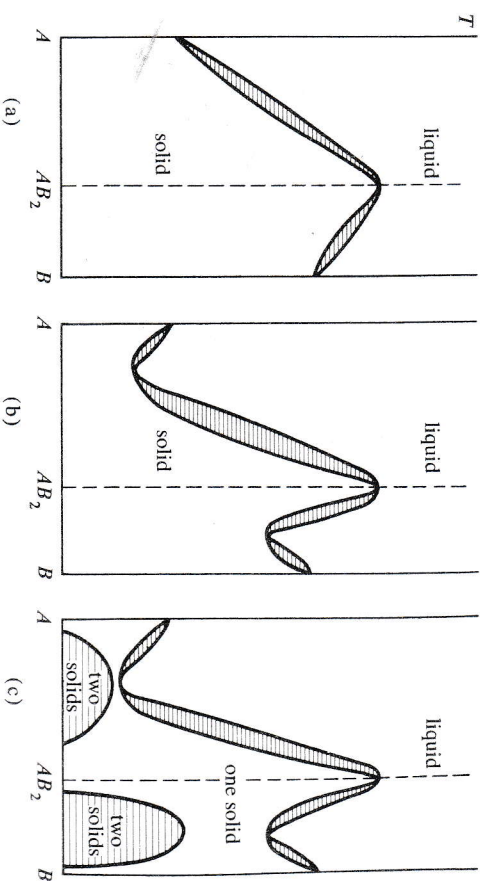


FIGURE 6-60. The development of a complex phase diagram from an elementary one, with extreme negative deviation leading to intermediate compound formation (a), and solid phase immiscibility (c).

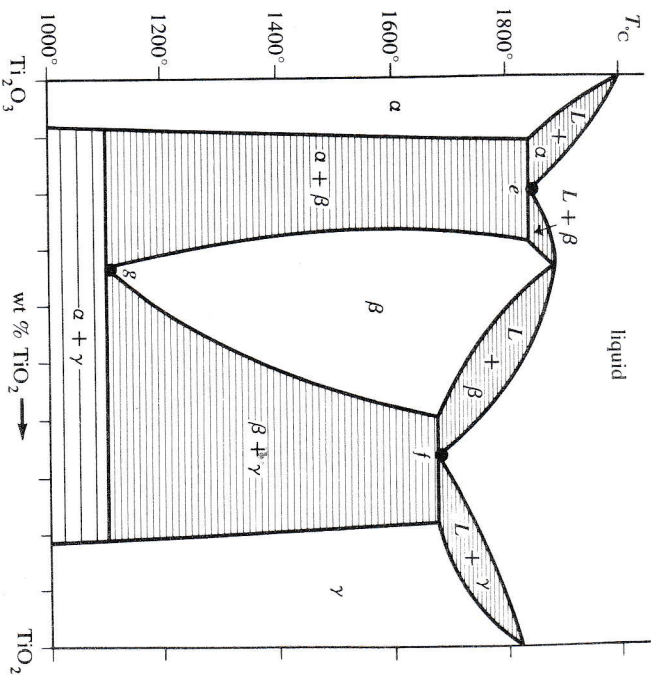


FIGURE 6-61. The  $\text{Ti}_2\text{O}_3$ - $\text{TiO}_2$  portion of the full Ti-O phase diagram, showing two eutectic points *e* and *f* and a eutectic point *g*. This diagram can be thought of as the next logical step in the sequence begun in Figure 6-60.

are two eutectic points  $e$  and  $f$  and a eutectoid point at  $g$  where, if equilibrium occurred quickly, one could observe the conversion of phase  $\beta$  to  $\alpha$  and  $\gamma$ . Just as the type structure for the  $\alpha$  phase is  $Ti_2O_3$  and that of  $\gamma$  is  $TiO_2$  although the exact compositions can vary widely, so the type formula for the  $\beta$  phase is  $Ti_3O_5$ .

Water and the various crystalline hydrates of sulfuric acid form the complex diagram of Figure 6-62. As sulfuric acid is added to water, the freezing point falls to a eutectic point at  $-70^\circ C$  with three phases present: freezing point solution, and solid tetrahydrate. As more acid is added, the ice, a 10% acid solution, and solid tetrahydrate. As more acid is added, the freezing point rises to  $-25^\circ C$ , the melting point of pure crystalline tetrahydrate. This sort of behavior occurs with each of the other hydrated forms, which can be considered as pure compounds in a diagram like Figure 6-58. The eutectic point in aqueous solutions is often called the cryohydric point, and the eutectic mixture, a cryohydrate.

The Na-K system (Figure 6-63) shows an important variation, incongruent melting at a peritectic point  $p$ . This diagram is to Figure 6-57 as the Cd-Bi diagram was to the Ag-Cu. Na and K form an intermediate compound  $Na_2K$  which is insoluble in either the Na or the K lattice. Pure  $Na_2K$  melts at  $6.6^\circ C$  to form solid Na and a liquid poorer in Na than the original solid:

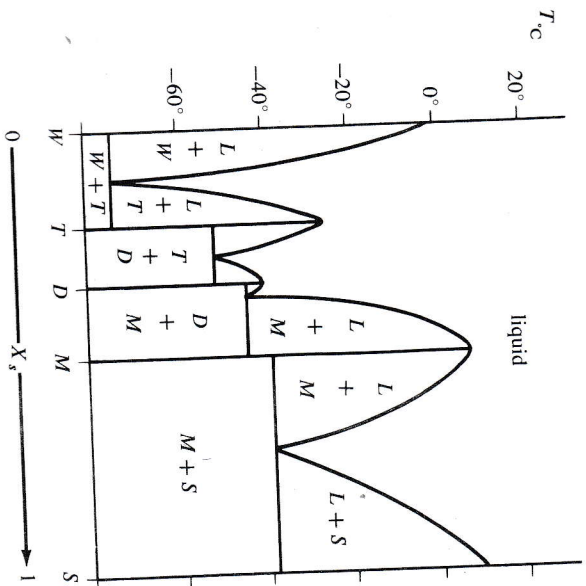


FIGURE 6-62. The phase diagram for the system of water (W) and sulfuric acid (S). Intermediate crystal forms are the monohydrate (M), dihydrate (D), and trihydrate (T) of sulfuric acid. This diagram can be thought of as a fourfold repetition of Figure 6-21 or 6-58.

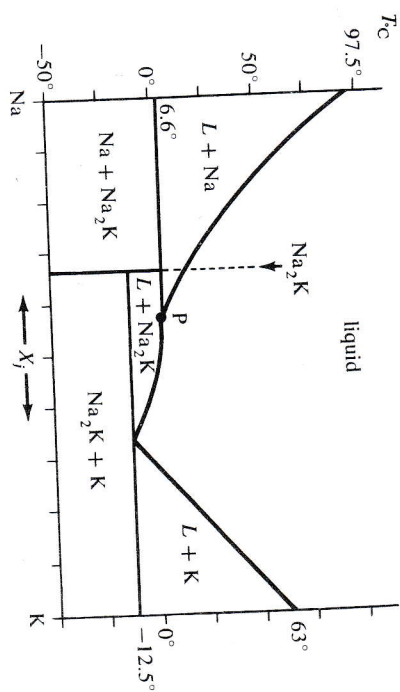


FIGURE 6-63. The Na-K system, with an intermediate compound  $Na_2K$  which melts incongruently at its peritectic point  $p$ . (From Hansen.)

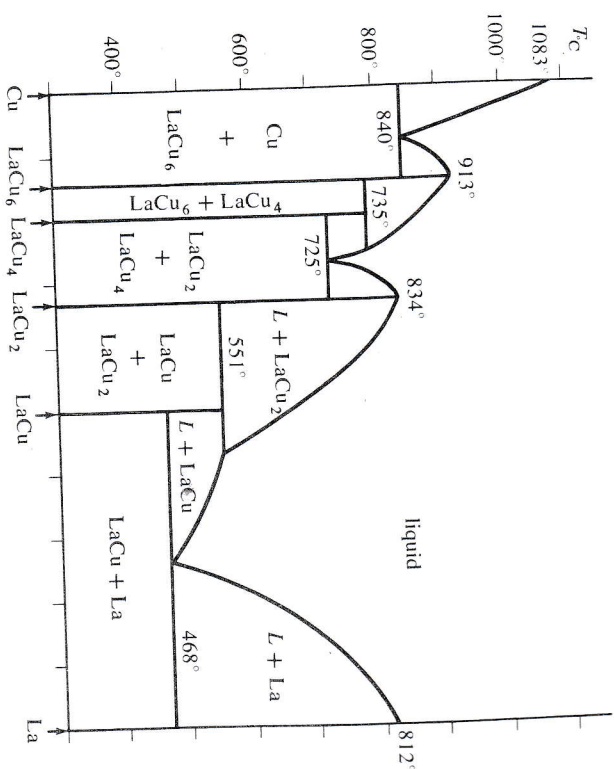


FIGURE 6-64. A compound phase diagram of Cu, La, and four intermediate compounds, all mutually insoluble in the solid phase. This diagram can be considered as being built up from simple diagrams such as Figures 6-58 and 6-63.





With three phases, the system will remain at the peritectic temperature of 6.6°C until the last  $\text{Na}_2\text{K}$  is gone.

Copper and lanthanum form no less than four intermediate compounds, all insoluble with one another, two of them melting eutectically and two peritectically (Figure 6-64). The interpretation of this phase diagram should now be obvious.

Whatever the nature of the solid compatibility, the liquid or melt is usually completely miscible. But for the ice-phenol system (Figure 6-65) this is not so. If a one-phase solution at  $a$  is cooled to  $b$ , the solubility limit is reached and two liquid phases separate. The composition of one falls along the curve toward  $d$ , and the other toward point  $e$ . At this point, solid phenol begins crystallizing out, and continues to do so until the last of the phenol-rich liquid phase at  $e$  is gone. The phenol-poor liquid and solid phenol then coexist in a normal way down to a true eutectic at point  $g$ .

The postgraduate course in this discussion of complex diagrams is the important Cu-Zn system, which includes all of the brasses. Its phase

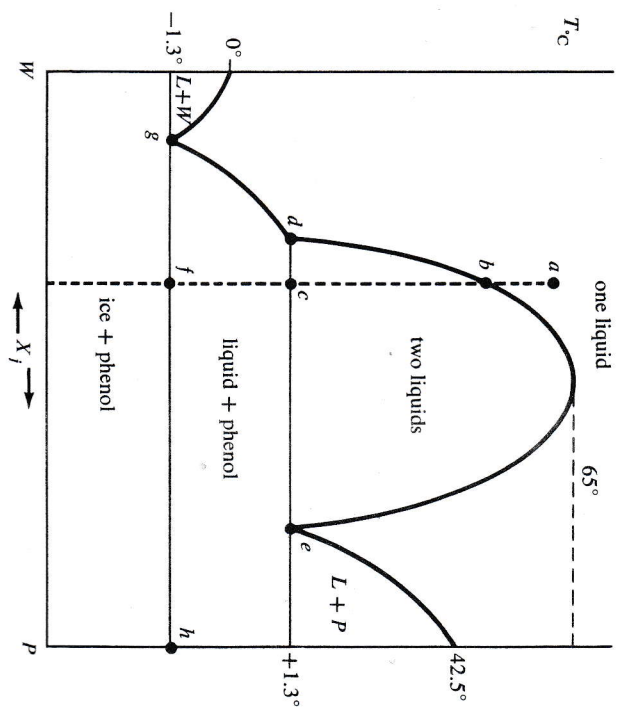


FIGURE 6-65. Partial liquid miscibility after melting: the system of water (W) and phenol (P). With the relationship between this figure and Figure 6-25 as a guide, the solid liquid equilibrium surfaces could be added to the grand phase diagram of Figure 6-45. How would they change with pressure, the axis normal to the page?

diagram, worked out patiently by a great many people over a great many years, is shown in Figure 6-66. There are six pure phases:  $\alpha$ ,  $\beta$ ,  $\gamma$ ,  $\delta$ ,  $\epsilon$ , and  $\eta$ .  $\alpha$  is the ccp lattice of pure Cu, and  $\eta$  is the hcp lattice of pure Zn.  $\beta$ -brass, the roughly equimolar form, is bcc with Cu and Zn atoms scattered at random throughout the lattice. The  $\beta'$  form below about 455°C is an ordered region in which all of the Cu atoms occupy the corners of the bcc lattice and the Zn atoms, the centers. This is the order-disorder transition discussed in connection with second order phase transitions, Section 5-6. Phase  $\gamma$  is a distorted bcc lattice with 52 atoms in a macrocell and the type composition  $\text{Cu}_5\text{Zn}_8$ . Phase  $\delta$  is bcc again, and  $\epsilon$  is hcp but with different lattice constants than the  $\eta$  form of nearly pure Zn.

Each of the solids except  $\alpha$  decomposes peritectically to give liquid and the next form richer in Cu. There are no eutectic points, but there are two eutectoid points, one near 250° for the reaction

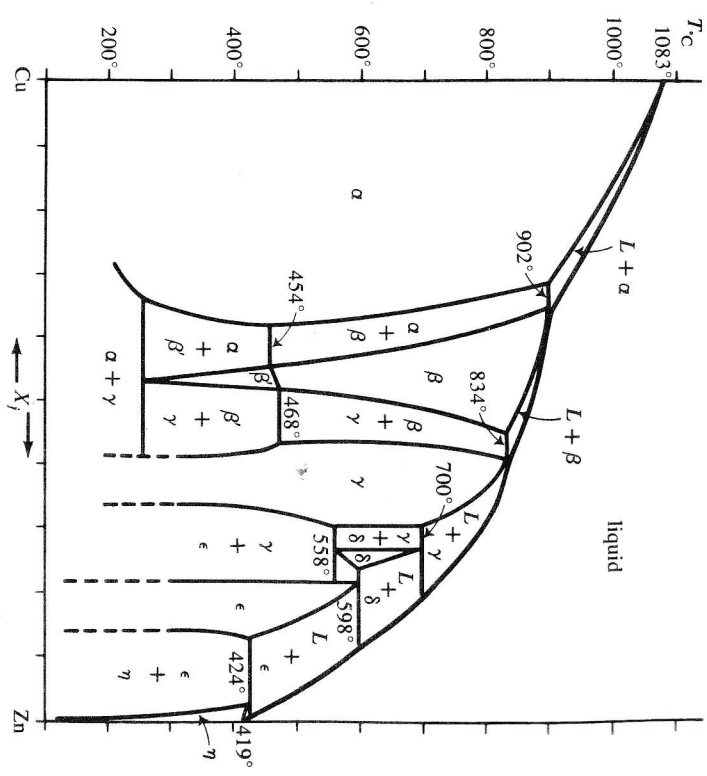


FIGURE 6-66. The Cu-Zn system of the brasses. For discussion, see text. (From Hansen.)



and another at 558° for

$$\delta = \gamma + \epsilon \quad (6-97)$$

The commercially important brasses are 30–33% Zn, in the  $\alpha$  phase near the  $\alpha$ - $\beta$  two-phase solubility boundary. Ordinary annealing at 600–650°C does not involve a phase change, but instead gives the grains a chance to grow and to make the metal more ductile. If a very high-Zn brass is then cooled to room temperature, it will enter a metastable two-phase zone, and very slow equilibration from  $\alpha$  to a mixture of  $\alpha$  and  $\gamma$  will take place.

### Moly-B Disaster

An expensive example of the perils of ignoring phase diagrams was provided once in the aerospace industry when an engineer decided to use a new \$500 molybdenum crucible (melting point, 2620°C) to melt powdered boron (melting point, 2037°C) into a one-pound ingot. The crucible with its charge of powdered boron was placed in a radio frequency induction furnace, the system was evacuated, and the crucible and charge were heated. Up to about 1900°C all went well, but shortly thereafter the boron appeared to be melting a good bit below its normal melting point. At about 1960°C the liquid began pouring through the bottom of what had been a new crucible, and back at 25°C the engineer was left with boron-molybdenum alloy all over the floor of his furnace and a very expensive piece of molybdenum pipe. The offending phase diagram is shown in Figure 6-67.

### REFERENCES AND FURTHER READING

Many of the texts referred to in earlier chapters have material on solutions and on multicomponent phase diagrams. The Debye-Hückel theory is covered in Wall and in Lewis and Randall. In addition, the following four books are important for their treatment of phase diagrams and equilibria.

- A. Findlay, *The Phase Rule* (Dover, New York, 1951).  
 S. T. Bowden, *The Phase Rule and Phase Reactions* (Macmillan, London, 1945).  
 J. E. Ricci, *The Phase Rule and Heterogeneous Equilibrium* (Van Nostrand, Princeton, N.J., 1951).  
 M. Hansen, *Constitution of Binary Alloys* (McGraw-Hill, New York, 1958), 2nd ed.

### SOLUTIONS

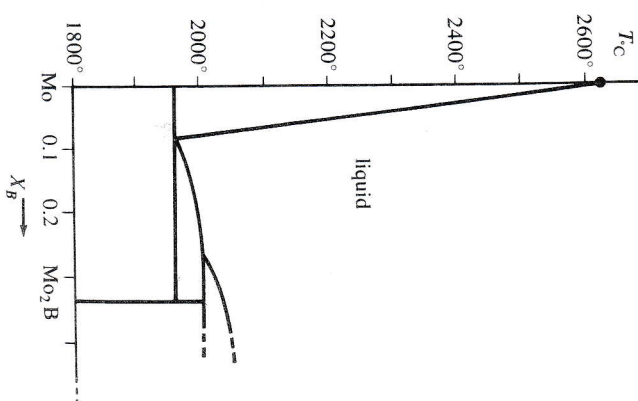


FIGURE 6-67. The Mo-rich half of the Mo-B phase diagram. (From Hansen.)

### EXERCISES

- 6-1. Naphthalene, which melts at 80°C, forms an ideal solution in benzene. If the heat fusion of naphthalene is 35.1 cal/g, calculate the solubility of naphthalene in benzene at 25°C. At what temperature would the solubility of naphthalene be 85 g/mole of benzene?
- 6-2. If 1.346 g of the protein  $\beta$ -lactoglobulin are dissolved in enough water to make up 100 cm<sup>3</sup> of solution at 25°C, then the osmotic pressure is observed to be 9.91 cm of water. Find a rough molecular weight for the protein.
- 6-3. (a) A solution of a polymer of high molecular weight dissolved in benzene shows an osmotic rise of 1.15 cm of benzene at 25°C. If  $K_f = 5.12$  for benzene, calculate the freezing point lowering of the solution and the vapor pressure lowering. The vapor pressure of pure benzene at this temperature is 94 mm of mercury. What do your results mean about the practicability of measuring freezing point lowering and vapor pressure lowerings of high polymer solutions?
- (b) The polymer solution above contains 3.15 g of polymer per liter of solution. A solution half as concentrated shows an osmotic rise of 0.51 cm at 25°C. Estimate the molecular weight of the polymer.







Plot the phase diagram for this system and identify all areas and phases. If a sample of over-all composition 40% by weight Sb were examined at 200°C, what components would be present and in roughly what proportions?

6-14. Phase diagrams such as the nicotine-water one of Figure 6-24 are sometimes a bit of a swindle because the pressure variable is inadequately controlled. Measurements of miscibility versus temperature by early workers were carried out in sealed capillaries, in which the pressure would rise with temperature. The only reason that such experiments now have any validity is that the dependence of miscibility on pressure is small within the pressure ranges involved. Data for Figure 6-24 were collected using 1-mm sealed glass capillaries made of special Jena glass; see C. S. Hudson, *Z. Phys. Chem.* **47**, 113 (1904). If the upper consolute temperature of 208°C occurs at a composition of 32% nicotine by volume, if the boiling point of nicotine at 1 atm pressure is 246°C, and if the vapor pressure of water at 208°C is 18.8 atm, estimate the true pressure within the capillary at the upper consolute point in Figure 6-24.

6-15. (a) A cup of coffee and a cup of tea are sitting side by side, each filled to the same point. One spoonful of coffee is transferred to the tea cup, thoroughly mixed in, and then one spoonful of the mixture is brought back to the coffee cup and mixed. At the end, which cup has more of the other cup's beverage in it? Note that there is a hard way and an easy way to solve this problem. Assume ideal solutions.

(b) Suppose that the liquids had been water and methyl ethyl ketone instead (Figure 6-25). What would your answer be? Is there now an easy shortcut? If not, what information would you need to solve the problem?

## Chapter 7

### THERMODYNAMICS AND LIVING SYSTEMS

It is possible to know thermodynamics without understanding it, or even to understand it without appreciating it. Thermodynamics should be more than a useful device for getting answers for a chemist; it should be a way of thought. For these three postulates and the definitions and ideas which go with them have a universality far beyond the tabulation of heats of reaction and predicting of equilibria. This chapter hopefully will give you some idea of the universality of thermodynamics, in applying it to that most interesting class of chemical systems, living organisms.

There is no intention here of providing a short course in biochemistry. Our only interest in specific reactions is in their illustration of a thermodynamic principle. We shall not hesitate where helpful to simplify or oversimplify to a point which would strike terror into the soul of a biologist. Nevertheless, the fact that thermodynamics deals with reality means that we will have to bring in a fair amount of biochemistry along the way. More background in possibly unfamiliar material which we shall gloss over quickly can be found in the references for further reading for this chapter. Lehninger and Klotz both have good treatments of free energy in biological reactions, and XII a classic treatment of entropy, time, and evolution which has never been bettered. Krebs and Kornberg will be the standard source for thermodynamic data, and Oparin and Bernal provide a good background in the origin of life.